การพัฒนาวิธีตรวจวัดโลหะหนักปริมาณน้อยมากด้วยซีเคว็นเชียลอินเจ็กชัน–แอโนดิกสทริปปิง
โวลแทมเมตรีโดยใช้ขั้วไฟฟ้าท่อนาโนคาร์บอนพิมพ์สกรีน

นางสาวอุทัยทิพย์ อินแจ้ง

METHOD DEVELOPMENT FOR THE DETERMINATION OF TRACE HEAVY
METALS BY SEQUENTIAL INJECTION-ANODIC STRIPPING
VOLTAMMETRY USING BISMUTH-COATED SCREEN PRINTED
CARBON NANOTUBE ELECTRODE

Miss Uthaitip  Injang

A Thesis Submitted in Partial Fulfillment of the Requirements
for the Degree of Master of Science Program in Chemistry
Department of Chemistry
Faculty of Science
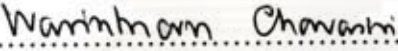Chulalongkorn University
Academic Year 2009

| Thesis Title | METHOD DEVELOPMENT FOR THE DETERMINATION OF TRACE HEAVY METALS BY SEQUENTIAL INJECTION-ANODIC STRIPPING VOLTAMMETRY USING BISMUTH-COATED SCREEN PRINTED CARBON NANOTUBE ELECTRODE |
| --- | --- |
| By | Miss Uthaitip Injang |
| Field of Study | Chemistry |
| Thesis Advisor | Associate Professor Orawon Chailapakul, Ph.D. |

Accepted by the Faculty of Science, Chulalongkorn University in Partial Fulfillment of the Requirements for the Master's Degree
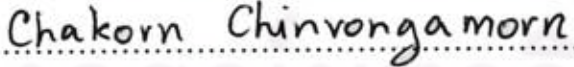
.................................... Dean of the Faculty of Science

(Professor Supot Hannongbua, Dr. rer. nat.)

THESIS COMMITTEE

.................................... Chairman

(Assistant Professor Warinthorn Chavasiri, Ph.D.)

.................................... Thesis Advisor

(Associate Professor Orawon Chailapakul, Ph.D.)

.................................... Examiner

(Assistant Professor Suchada Chuanuwatanakul, Ph.D.)

.................................... External Examiner

(Chakorn Chinvongamorn, Ph.D.)

อุทัยทิพย์ อินแจ้ง : การพัฒนาวิธีตรวจวัดโลหะหนักปริมาณน้อยมากด้วยซีเควินเชียล อินเจ็กชัน-แอโนดิกสทริปปิงโวลแทมเมตรีโดยใช้ขั้วไฟฟ้าท่อนาโนคาร์บอนพิมพ์สกรีน (METHOD DEVELOPMENT FOR THE DETERMINATION OF TRACE HEAVY METALS BY SEQUENTIAL INJECTION-ANODIC STRIPPING VOLTAMMETRY USING BISMUTH-COATED SCREEN PRINTED CARBON NANOTUBE ELECTRODE) อ. ที่ปรึกษาวิทยานิพนธ์หลัก : รศ.ดร.อรวรรณ ชัยลภากุล, ..67.. หน้า

งานวิจัยนี้ ได้พัฒนาวิธีการตรวจวัดโลหะหนักตะกั่ว แคดเมียม และสังกะสีที่ความเข้มข้น ต่ำๆ ในเวลาเดียวกัน ด้วยซีเควินเชียลอินเจ็กชัน-แอโนดิกสทริปปิงโวลแทมเมตรีโดยใช้ขั้วไฟฟ้าท่อ นาโนคาร์บอนพิมพ์สกรีนเคลือบด้วยบิสมัทเป็นขั้วไฟฟ้าใช้งาน แผ่นฟิล์มบิสมัทจะถูกเคลือบ ระหว่างการตรวจวัดบนขั้วไฟฟ้าใช้งานที่ผ่านการพิมพ์สกรีนแล้ว ศึกษาหาภาวะที่เหมาะสมในการ ทดลอง ได้แก่ อัตราส่วนของท่อนาโนคาร์บอนต่อหมึกคาร์บอน ความเข้มข้นของสารละลายบิสมัท ที่ใช้เคลือบ เวลาที่โลหะเข้าไปเกาะติด และอัตราการไหลของสารขณะทำการตรวจวัดที่ความ เข้มข้นของสารละลายอิเล็กโทรไลต์เกื้อหนุนกรดไฮโดรคลอริก 1 M ที่ภาวะเหมาะสม พบว่า ความสัมพันธ์เชิงเส้นตรงระหว่างความเข้มข้นกับสัญญาณอยู่ในช่วงความเข้มข้น 2-100 $\mu g\ L^{-1}$ ของโลหะตะกั่วและแคดเมียม และ 12-100 $\mu g\ L^{-1}$ ของโลหะสังกะสี ขีดจำกัดการตรวจวัดต่ำสุด ของตะกั่ว เท่ากับ 0.2 $\mu g\ L^{-1}$ , แคดเมียม เท่ากับ 0.8 $\mu g\ L^{-1}$ และสังกะสี เท่ากับ 11 $\mu g\ L^{-1}$ การตรวจวัดมีความถี่ในช่วง 10-15 ตัวอย่างต่อชั่วโมง วิธีการตรวจวัดแบบอัตโนมัตินี้มีสภาพไวต่อ การตรวจวัดสูง สามารถใช้ตรวจวัดปริมาณโลหะตะกั่ว แคดเมียม และสังกะสีในตัวอย่างสมุนไพร

ภาควิชา.......เคมี......... ลายมือชื่อนิสิต.....................................................

สาขาวิชา......เคมี......... ลายมือชื่อ อ.ที่ปรึกษาวิทยานิพนธ์หลัก........................

ปีการศึกษา...2552........

v

# # 5072579323: MAJOR CHEMISTRY
KEYWORDS: HEAVY METALS / SEQUENTIAL INJECTION ANALYSIS / ANODIC STRIPPING VOLTAMMETRY / CARBON NANOTUBE ELECTRODE

UTHAITIP INJANG : METHOD DEVELOPMENT FOR THE DETERMINATION OF TRACE HEAVY METALS BY SEQUENTIAL INJECTION-ANODIC STRIPPING VOLTAMMETRY USING BISMUTH-COATED SCREEN PRINTED CARBON NANOTUBE ELECTRODE. THESIS ADVISOR : ASSOC. PROF. ORAWON CHAILAPAKUL, Ph.D., ..67.. pp.

In this research, a method for the simultaneous determination of Pb (II), Cd (II), and Zn (II) at low $\mu g\ L^{-1}$ concentration levels by sequential injection analysis-anodic stripping voltammetry (SIA-ASV) using screen-printed carbon nanotube electrode (SPCNTE) was developed. A bismuth film was prepared by in situ plating of bismuth on the screen-printed carbon nanotubes electrode. Operational parameters such as ratio of carbon nanotubes to carbon ink, bismuth concentration, deposition time and flow rate during preconcentration step were optimized. Under the optimal conditions, the linear ranges were found to be 2-100 $\mu g\ L^{-1}$ for Pb (II) and Cd (II), and 12-100 $\mu g\ L^{-1}$ for Zn (II). The limits of detection ($S_{bl}/S=3$) were 0.2 $\mu g\ L^{-1}$ for Pb (II), 0.8 $\mu g\ L^{-1}$ for Cd (II) and 11 $\mu g\ L^{-1}$ for Zn (II). The measurement frequency was found to be 10-15 stripping cycle $h^{-1}$. The present method offers high sensitivity and high throughput for on-line monitoring of trace heavy metals. The practical utility of our method was also demonstrated with the determination of Pb (II), Cd (II), and Zn (II) by spiking procedure in herb samples.

Department : ..........Chemistry...... Student's Signature.....Uthaitip Injang.....
Field of Study : ......Chemistry...... Advisor's Signature.....Orawon Chaila.....
Academic Year : ....2009................

# ACKNOWLEDGEMENTS

# CONTENTS

# LIST OF TABLES

## LIST OF TABLES

# LIST OF FIGURES

# LIST OF ABBREVIATIONS

| | |
|---|---|
| A | Ampere |
| AAS | Atomic Absorption Spectroscopy |
| Ag | Silver |
| Ag/AgCl | Silver/Silver Chloride |
| ASV | Anodic Stripping Voltammetry |
| Bi | Bismuth |
| BiF | Bismuth Film |
| BiFE | Bismuth Film Electrode |
| Cd | Cadmium |
| CNT | Carbon Nanotube |
| CE | Counter Electrode |
| °C | Degree Celsius |
| E | Potential |
| $E_{1/2}$ | Half-wave Potential |
| FTIR | Fourier Transform Infrared |
| GC | Glassy Carbon |
| i | Current |
| M | Molar |
| mL | Milliliter |
| min | Minute |
| MS | Mass spectrometry |
| MWNT | Multi-Walled Carbon Nanotube |
| Pb | Lead |
| Pt | Platinum |
| RE | Reference Electrode |
| s | Second |
| SIA | Sequential Injection Analysis |
| SPCE | Screen Printed Carbon Electrode |
| SPC | Screen Printed Carbon Nanotube Electrode |

| | |
|---|---|
| SWASV | Square Wave Anodic Stripping Voltammetry |
| SWCNT | Single-Walled Carbon Nanotube |
| V | Volt |
| v/v | Volume by Volume |
| μA | Microampere |
| μL | Microliter |
| We | Working Electrode |
| Zn | Zinc |
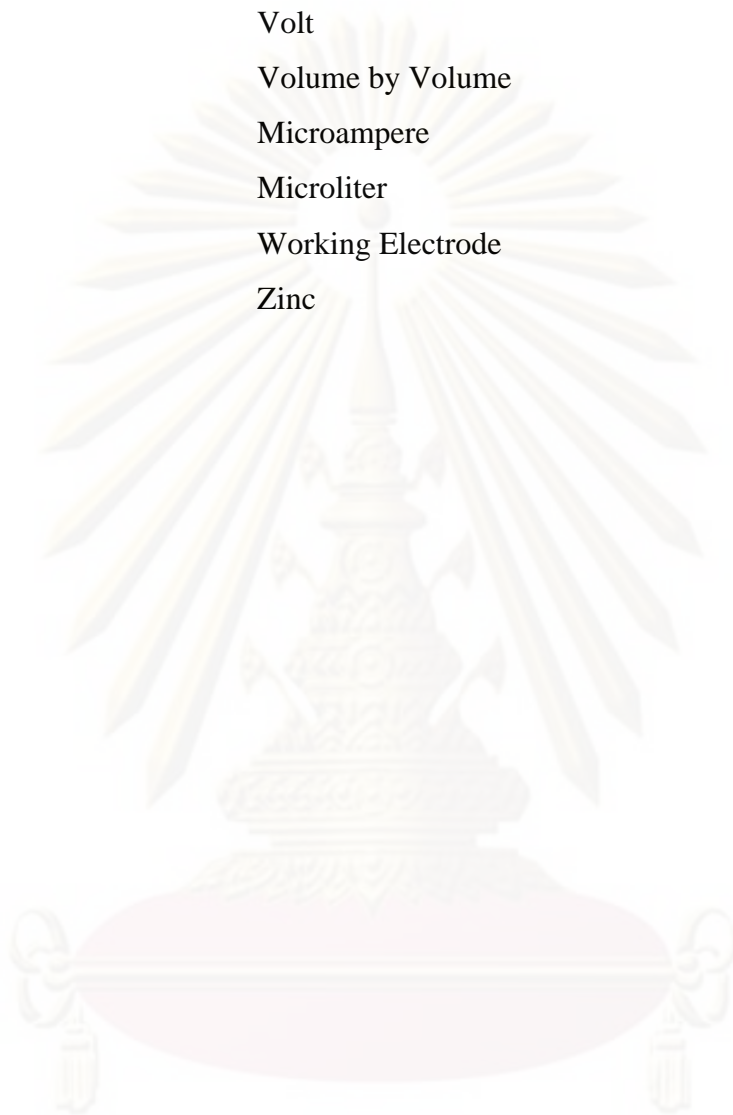
# CHAPTER I

# INTRODUCTION

## 1.1   Introduction

Nowadays, herbal medicines are a common form of alternative medicine because they are perceived as being natural and safe.  One well-known herb in southern Asia is Andrographis.  It has been reported to possess antihepatotoxic, antibiotic, antimalarial, antihepatitic, antithrombogenic, anti-inflammatory, and anti-snake venom.  It has also the potential for being developed as a cancer therapeutic agent.  Even though herbal medicines have many significant benefits, they still have important problems including contamination with heavy metals [1].  Herbal medicines contaminated with heavy metals arise from contaminated agricultural lands and/or the production process.  Hence, the determination of heavy metal content in herb is important for both toxicological and acceptance criteria.  Several analytical techniques such as atomic absorption spectrometry (AAS) [2,3], inductive coupled plasma atomic emission spectrometry (ICP-AES) [4], inductively coupled plasma mass spectrometry (ICP-MS) [5,6], and anodic stripping voltammetry (ASV) [1,7-9] have been used for heavy metal analysis.  One of the most powerful methods for several trace heavy metals analysis is ASV due to its sensitivity and low instrument cost.  Stripping voltammetry has been adapted to flow systems with the intention to exploit the advantage conferred by on-line analysis.  In order to overcome these shortcomings, flow-injection analysis (FIA) systems have been reported for stripping analysis that provide lower sample consumption and are more suitable for on-line mixing of sample and reagent.  The limitations of FIA itself (including multichannel manifolds, the need for continuous pumping of solutions and increased consumption of reagents) have been solved by replacing with Sequential injection analysis (SIA) [10,11].  Sequential injection analysis (SIA), consisting of multiposition valve and syringe pump, is the next generation of flow injection analysis system.  SIA has great

potential for coupling with ASV due to the simplicity and convenience for the sample manipulation [12]. Moreover, SIA-ASV can be automated.

Mercury electrodes have been traditionally used for ASV or potentiometric stripping analysis [13] to obtain high sensitivity, reproducibility, and a wide cathodic potential range. Unfortunately, the toxicity of mercury and its difficulties in handling, storage, and disposal severely restrict its use as an electrode material. Recently, the bismuth film electrode was introduced for the electrochemical measurements of heavy metals because it possesses behavior similar to the mercury electrode and it is more environmentally friendly [14]. The bismuth (Bi) can be constructed by electrode position on substrates including glassy carbon [8], screen-printed carbon ink (SPCE) [15]. Carbon nanotubes (CNTs) have been proven to possess potential for heavy metals analysis due to their high electrical conductivity, high surface area, significant mechanical strength, and good chemical stability. Therefore, the fabrication of screen-printed carbon nanotubes electrode (SPCNTE) is attractive. In effort to improve the sensitivity of heavy metals by electrochemical analysis, Bi-SPCNTE was used as the working electrode [16,17].

## 1.2    Literature Review

X. He *et al.* [1] developed Nafion-coated bismuth film electrodes to determine Pb (II) and Cd (II) in herbal medicines commercially available in China by differential pulse anodic stripping voltammetry. Various experimental parameters, which influenced the response of the NCBFE to these metals in real samples, were optimized. The results showed that there were well-defined peaks of Pb and Cd in herb samples at deposition potential of -1.2 V and deposition time of 300 s. The analytical performance of the NCBFE was evaluated in the presence of dissolved oxygen, with the determination limits of 0.35 µg L$^{-1}$ for Pb and 0.72 µg L$^{-1}$ for Cd and recoveries of 87.8%-105.4% for Pb and 89.5%-108.5% for Cd obtained from different samples. The Pb and Cd concentration in the studied samples have been also determined by graphite furnace atomic absorption spectrometry (GFAAS), suggesting that there was a satisfactory agreement between the two techniques, with relative errors lower than 6.5% in all cases. The great advantages of the proposed method

over the spectroscopic method were characterized by its simplicity, selectivity and short analysis time, simultaneous analysis of different metals and cost-efficiency.

G. Kefala *et al*. [8] investigated the utility of Nafion coated BiFEs as flow through sensors for the determination of trace metals by SIA-ASV. The polymeric Nafion coating was initially plated on a glassy carbon electrode forming part of the flow through electrochemical cell. The subsequent steps of the bismuth layer generation, analyte preconcentration, voltammetric measurement and electrode cleaning were conducted on-line. For a sample volume of 1.2 mL, the limits of detection (at S/N=3) were 2 µg L$^{-1}$ for Cd (II) and Pb (II) and 6 µg L$^{-1}$ for Zn (II), the coefficients of variation at 20 µgL$^{-1}$ were 5.1% for Cd (II), 5.9% for Pb (II) and 6.2% for Zn (II) and the measurement frequency was between 10 and 20 h$^{-1}$. It is demonstrated that the polymer coated BiFEs, combined with SIA, can provide an environmentally friendly, sensitive and robust tool to perform rapid and cost efficient on-line monitoring of trace metals by ASV, even in the presence of surface active compounds.

J. Wang *et al.* [9] prepared bismuth film electrodes by adding 400 µg L$^{-1}$ bismuth(III) directly to the sample solution and simultaneously depositing the bismuth and target metals on the glassy carbon or carbon fiber substrate. Stripping voltammetric measurements of microgram per liter levels of cadmium, lead, thallium, and zinc in nondeaerated solutions yielded well-defined peaks, along with a low background, following short deposition periods. Detection limit of 1.1 and 0.3 µg L$^{-1}$ lead are obtained following 2 and 10 min deposition, respectively. Changes in the peak potentials (compared to those observed at mercury electrodes) offer new selectivity dimensions. Scanning electron microscopy sheds useful insights into the different morphologies of the bismuth deposits on the carbon substrates. The in situ bismuth plated electrodes exhibit a wide accessible potential window (-1.2 to -0.2 V) that permits quantitation of most metals measured at mercury electrodes. Numerous key experimental variables have been characterized and optimized. High reproducibility was indicated from the relative standard deviations (2.4 and 4.4%) for 22 repetitive measurements of 80 µg L$^{-1}$ cadmium and lead, respectively.

A. Economou *et al.* [10] describe an automated stripping analyzer operating on a hybrid flow-injection/sequential-injection (FIA/SIA) mode and utilizing a bismuth film electrode (BiFE) as a flow-through sensor for on-line stripping voltammetry of trace metals. The instrument combines the advantages of FIA and SIA and is characterized by simplicity, low-cost, rapidity, versatility and low consumption of solutions. The proposed analytical flow methodology was applied to the determination of Cd (II) and Pb (II) by anodic stripping voltammetry (ASV). The steps of the rather complex experimental sequence were conducted on-line and the critical parameters related to the respective analytical procedures were investigated. A accumulation time of 180 s the limits of detection for Cd (II) and Pb (II) were 2 and 1 $\mu$g L$^{-1}$, respectively (S$_{bl}$/N=3) and the relative standard deviations were 5.3% and 4.7%, respectively (n=8). The measurement frequency ranged between 15 and 20 stripping cycles h$^{-1}$. The results indicate that the BiFE is well suited as a flow-through detector for on-line stripping analysis and, by virtue of its low toxicity, can serve as a viable alternative to mercury-based flow-through electrodes.

E.A. Hutton *et al.* [14] developed method for the measurement of tin using anodic stripping voltammetry in combination with catechol as a complexing agent. The procedure involves simultaneous in situ formation of the bismuth film electrode on a glassy carbon substrate electrode, together with electrochemical deposition of tin, in a non-deaerated model solution containing bismuth ions, catechol as complexing agent and the metal analyte, followed by an anodic stripping scan. The BiFE is characterized by an attractive electroanalytical performance, with two distinct voltammetric stripping signals corresponding to tin, accompanied with low background contributions. Several experimental parameters were optimized, such as concentration of bismuth ions and catechol, deposition potential, deposition time and pH of the model solution. In addition, a critical comparison is given with bare glassy carbon and mercury film electrodes, revealing the superior characteristics of BiFE for measurement of tin. BiFE exhibited highly linear behavior in the examined concentration range from 1 to 100 $\mu$g L$^{-1}$ of tin (R$^2$ = 0.997), an LOD of 0.26 $\mu$g L$^{-1}$ tin, and good reproducibility with a calculated R.S.D. of 7.3% for 10 $\mu$g L$^{-1}$ tin

(n=10).  As an example, the practical applicability of BiFE was tested with the measurement of tin in a real sample of seawater.

S. Chuanuwatanakul *et al.* [15] developed method for the on-line simultaneous determinations of Pb (II), Cd (II) and Zn (II) on in situ plated Bi-SPCE using a sequential injection system coupled with square-wave anodic stripping voltammetry (SIA-SWASV).  Bi (III) and analyte metal ions were on-line deposited onto a SPCE at -1.4 V vs. Ag/AgCl for 180 s.  At a stopped flow, a square-wave voltammogram was recorded from -1.3 to 0 V vs. Ag/AgCl.  The experimental conditions were optimized.  Under the optimum conditions, the linear ranges were 0-70 $\mu$g L$^{-1}$ for Pb (II) and Cd (II), and 75-200 $\mu$g L$^{-1}$ for Zn (II).  The limits of detection ($S_{bl}$/N=3) were obtained at concentrations as low as 0.89 $\mu$g L$^{-1}$ for Pb (II) and 0.69 $\mu$g L$^{-1}$ for Cd (II) for a 180 s deposition time.  The proposed method was applied to the determination of Pb (II), Cd (II) and Zn (II) in water samples with satisfactory results.

G.H. Hwang *et al.* [16] prepared the CNT electrode by screen-printing technique.  This technique was well established for the production of low cost, reproducible and sensitive electrochemical sensors.  The electrochemical characteristics of CNT electrode were compared with glassy carbon, activated carbon and graphite electrodes.  It was clear that the CNT-based electrode had much better sensitivity than the other electrodes for anodic stripping voltammetry.  The bismuth-modified carbon nanotube electrode (Bi-CNT electrode) was employed for the determination of trace lead, cadmium and zinc.  Bismuth film was prepared by in situ plating of bismuth onto the screen-printed CNT electrode.  Operational parameters such as preconcentration were optimized for the purpose of determining trace metals in 0.1 M acetate buffer solution (pH 4.5).  The simultaneous determination of lead, cadmium and zinc was performed by square wave anodic stripping voltammetry.  The Bi-CNT electrode presented well-defined, reproducible and sharp stripping signals.  The peak current response increased linearly with the metal concentration in a range of 2-100 $\mu$g L$^{-1}$.  The limit of detection was 1.3 $\mu$g L$^{-1}$ for lead, 0.7 $\mu$g L$^{-1}$ for cadmium and 12 $\mu$g L$^{-1}$ for zinc ($S_{bl}$/N=3).  The Bi-CNT electrode was successfully applicable to analysis of trace metals in real environments.

J. Wang *et al.* [18] reported the simultaneous determination of Cd (II), Pb (II) and Zn (II) at the low µg $L^{-1}$ concentration levels by square wave anodic stripping voltammetry (SWASV) on a bismuth film electrode (BFE) plated in situ. The metal ions and bismuth were simultaneously deposited by reduction at -1.4 V on a rotating glassy carbon disk electrode. Then, the preconcentrated metals were oxidised by scanning the potential of the electrode from -1.4 to 0 V using a square wave waveform. The stripping current arising from the oxidation of each metal was related to the concentration with the view to apply this type of voltammetric sensor to real samples containing low concentrations of metals. Using the selected conditions, the limits of detection were 0.2 µg $L^{-1}$ for Cd and for Pb and 0.7 µg $L^{-1}$ for Zn at a preconcentration time of 10 min. Finally, BFE's were successfully applied to the determination of Pb and Zn in tapwater and human hair and the results were in satisfactory statistical agreement with atomic absorption spectroscopy (AAS).

## 1.3 Objective and Scopes of the Thesis

The objective of this research was to develop a highly sensitive, rapid, and low-cost automatic method for the determination of trace heavy metals by SIA-ASV using Bi-SPCNTE. The thesis was divided into four parts. For the first part, the comparison of the electrochemical response between Bi-SPCNTEs and Bi-SPCEs was studied to gain better conditions for determination of Pb(II), Cd(II), and Zn at low µg $L^{-1}$ concentration levels. The second part was the main part of the thesis involving with the optimization of operation conditions such as percentages of CNTs to carbon ink used for the electrode preparation, effect of deposition time and effect of flow rate. The third part, the analytical performance of the Bi-SPCNTEs was investigated. Finally, the application of the proposed method to determine heavy metals in herb samples was performed.

# CHAPTER II

# THEORY

For the understanding of this thesis, the definitions and theories of the following terms will be described: heavy metals, Andrographis Paniculata, electrochemical techniques, carbon nanotube (CNT), screen-printed carbon (SPC), flow injection analysis (FIA) and sequential injection analysis (SIA).

## 2.1. Heavy Metals [19]

Heavy metals are of great significance in chemistry and toxicology because of their toxicity at low levels and tendency to accumulate in human organs[19].

Some characteristic symptoms of toxicity, deficiency and the recommended daily allowances of some heavy metals are listed in the Table 2.1, Table 2.2 and Table 2.3, respectively.

**Table 2.1** Toxicological symptoms of some toxic heavy metals.

| Metal | Toxicological symptoms |
|-------|------------------------|
| Cd | embrittlement of bones and extremely painful deformations of the skeleton (Itai-Itai desease) |
| Pb | osteoporosis, hematological and gastrointestinal symptoms such as colic, anemia, neurotoxic symptoms especially a mental retardation in children |

**Table2.2** Some characteristic symptoms of chemical element deficiency in human.

| Deficient element | Typical deficiency symptoms |
| --- | --- |
| Ca | retarded skeletal growth |
| Mg | muscle cramps |
| Fe | anemia, disorders of the immune system |
| Zn | skin damage, stunted growth, retarded sexual maturation |
| Cu | artery weakness, liver disorders, secondary anemia |
| Mn | infertility, impaired skeletal growth |
| Mo | retardation of cellular growth, propensity for caries |
| Co | pernicious anemia |
| Ni | growth depression, dermatitis |
| Cr | diabetes symptoms |

**Table2.3** The recommended daily allowances of elements for adults and infants.

| element | Recommended daily allowances (in mg) | |
| --- | --- | --- |
| | adults | infant |
| K | 2000-5500 | 530 |
| Na | 1100-3300 | 260 |
| Ca | 800-1200 | 420 |
| Mg | 300-400 | 60 |
| Zn | 15 | 5 |
| Fe | 10-20 | 7.0 |
| Mn | 2.0-5 | 1.3 |
| Cu | 1.5-3 | 1.0 |
| Mo | 0.075-0.250 | 0.06 |
| Cr | 0.05-0.2 | 0.04 |
| Co | 0.2 (vitamin B12) | 0.001 |

### 2.1.1 Cadmium

Cadmium is a chemical element with a symbol Cd and atomic number 48. A relatively abundant, soft, bluish-white, transition metal, cadmium is know to cause cancer and occurs with zinc ores. It is used largely in batteries and pigmentsm, for example in plastic products.

Cadmium is an occupational hazard associated with industrial processes such as metal plating and the production of nickel-cadmium batteries, pigments, plastics, and other synthetics. The primary route of exposure in industrial settings is inhalation. Inhalation of cadmium-containing fumes can result initially in metal fume fever but may progress to chemical pneumonitis, pulmonary edema, and death.

### 2.1.2 Lead

Lead is a main group element with a symbol Pb and atomic number 82. It is a soft, malleable poor metal, also considered to be one of the heavy metals. Lead is a poisonous metal that can damage nervous connections (especially in young children) and cause blood and brain disorders. Because of its low reactivity and solubility lead poisoning usually only occurs in cases when the lead is dispersed, like when sanding lead based paint, or long term exposure in the case of pewter tableware. Long term exposure to lead or its salts (especially soluble salts or the strong oxidant $PbO_2$) can cause nephropathy, and colic-like abdominal pains. The concern about lead's role in cognitive deficits in children has brought about widespread reduction in its use (lead exposure has been linked to schizophrenia). Most cases of adult elevated blood lead levels are workplace-related. High blood levels are associated with delayed puberty in girls. Older houses may still contain substantial amounts of lead paint. White lead paint has been withdrawn from sale in industrialized countries, but the yellow lead chromate is still in use; for example, Holland Colours Holcolan Yellow. Old paint should not be stripped by sanding, as this produces inhalable dust.

### 2.1.3 Zinc

Zinc is a metallic chemical element with the symbol Zn and atomic number 30. Even though zinc is an essential requirement for a healthy body, too much zinc can be harmful. Excessive absorption of zinc can also suppress copper and iron absorption. The free zinc ion in solution is highly toxic to plants, invertebrates, and even vertebrate fish. The Free Ion Activity Model (FIAM) is well-established in the literature, and shows that just micromolar amounts of the free ion kills some organisms. A recent example showed 6 micromolar killing 93% of all Daphnia in water. The free zinc ion is also a powerful Lewis acid up to the point of being corrosive. Stomach acid contains hydrochloric acid, in which metallic zinc dissolves readily to give corrosive zinc chloride. Swallowing a post 1982 American one cent piece (97.5% zinc) can cause damage to the stomach lining due to the high solubility of the zinc ion in the acidic stomach. Zinc toxicity, mostly in the form of the ingestion of US pennies minted after 1982, is commonly fatal in dogs where it causes a severe hemolytic anemia. In pet parrots zinc is highly toxic and poisoning can often be fatal.

### 2.2 Andrographis paniculata

Andrographis paniculata is a herbaceous plant in the family *Acanthaceae*, native to India and Sri Lanka. It is widely cultivated in southern Asia, where it is used to treat infections and some diseases, often being used before antibiotics were created. Mostly the leaves and roots were used for medicinal purposes. As shown in figure 2.1



**Figure 2.1** Andrographis Paniculata

Since ancient times, *A. paniculata* is used in traditional Siddha and Ayurvedic systems of medicine as well as in tribal medicine in India and some other countries for multiple clinical applications. The therapeutic value of Kalmegh is due to its mechanism of action which is perhaps by enzyme induction. The plant extract exhibits antityphoid and antifungal activities. Kalmegh is also reported to possess antihepatotoxic, antibiotic, antimalarial, antihepatitic, antithrombogenic, anti-inflammatory, anti-snake venom, and antipyretic properties to mention a few, besides its general use as an immunostimulant agent. A recent study conducted at Bastyr University, confirms the anti-HIV activity of andrographolide.

## 2.3 Electrochemical Techniques [20-22]

Electrochemistry encompasses chemical and physical processes that involve the transfer of charge. There are two categories of electrochemical processes, potentiometric and electrolytic methods, that are applied to quantitative measurements. Potentiometry is the field of electroanalytical chemistry in which potential is measure under the conditions of no current flow. The measured potential may then be used to determine the analytical quantity of interest, generally the concentration of some component of the analyte solution. Unlike potentiometry, where the free energy contained within the system generates the analytical signal, electrolytic methods are an area of electroanalytical chemistry in which an external source of energy is supplied to drive an electrochemical reaction which would not normally occur. The externally applied driving force is either an applied potential or current. When potential is applied, the resultant current is the analytical signal; and when current is applied, the resultant potential is the analytical signal. Techniques which utilize applied potential are typically referred to as voltammetric methods while those with applied current are referred to as galvanostatic methods. Unlike potentiometric measurements, which employ only two electrodes, voltammetric measurements utilize a three electrode electrochemical cell. The use of three electrodes (working, auxillary, and reference) along with the potentiostat instrument allows accurate application of potential functions and the measurement of the resultant current. The different voltammetric techniques are distinguished from each

other primarily by the potential function that is applied to the working electrode to drive the reaction, and by the material used as the working electrode. Although many electrochemical methods are available nowadays, only anodic stripping voltammetry (ASV) are used in this thesis.

### 2.3.1 Voltammetry [23-25]

Voltammetry comprises a group of the electroanalytical methods in which information about the analyte is derived from the measurement of current as a function of applied potential. It is based on the measurement of a current that develops in an electrochemical cell under conditions of complete concentration of polarization of working electrode. In the presence of the electroactive (reducible or oxidizable) species, a current will be recorded when the applied potential becomes sufficiently negative or positive for it to electrolyze. The recording result is called a voltammogram. The potential excitation signal is imposed on an electrochemical cell containing an electrode. Three waveforms of most common excitation signals used in voltammetry are shown in Figure 2.2 . The classical voltammetric excitation signal is a linear scan shown in Figure 2.2 (a). The potential applied to the cell of this excitation increases linearly as a function of time. The two pulse excitation signals are shown in Figure2.2 (b) and2.2 (c). The current responses of the pulse type are measured at various times during the lifetime of these pulses. Voltammetry is widely used for the fundamental studies of oxidation and reduction processes in various media, adsorption process on electrode surfaces, and electron transfer mechanisms at electrode surfaces. In the mid-1960s, several major modifications of classical voltammetric techniques were developed that enhanced the sensitivity and selectivity of the method.

| Name | Waveform | Type of voltammetry |
|------|----------|---------------------|
| (a) Linear scan |  | Polarography, Hydrodynamic voltammetry |
| (b) Differential pulse |  | Differential pulse Polarography |
| (c) Square wave |  | Square wave voltammetry |
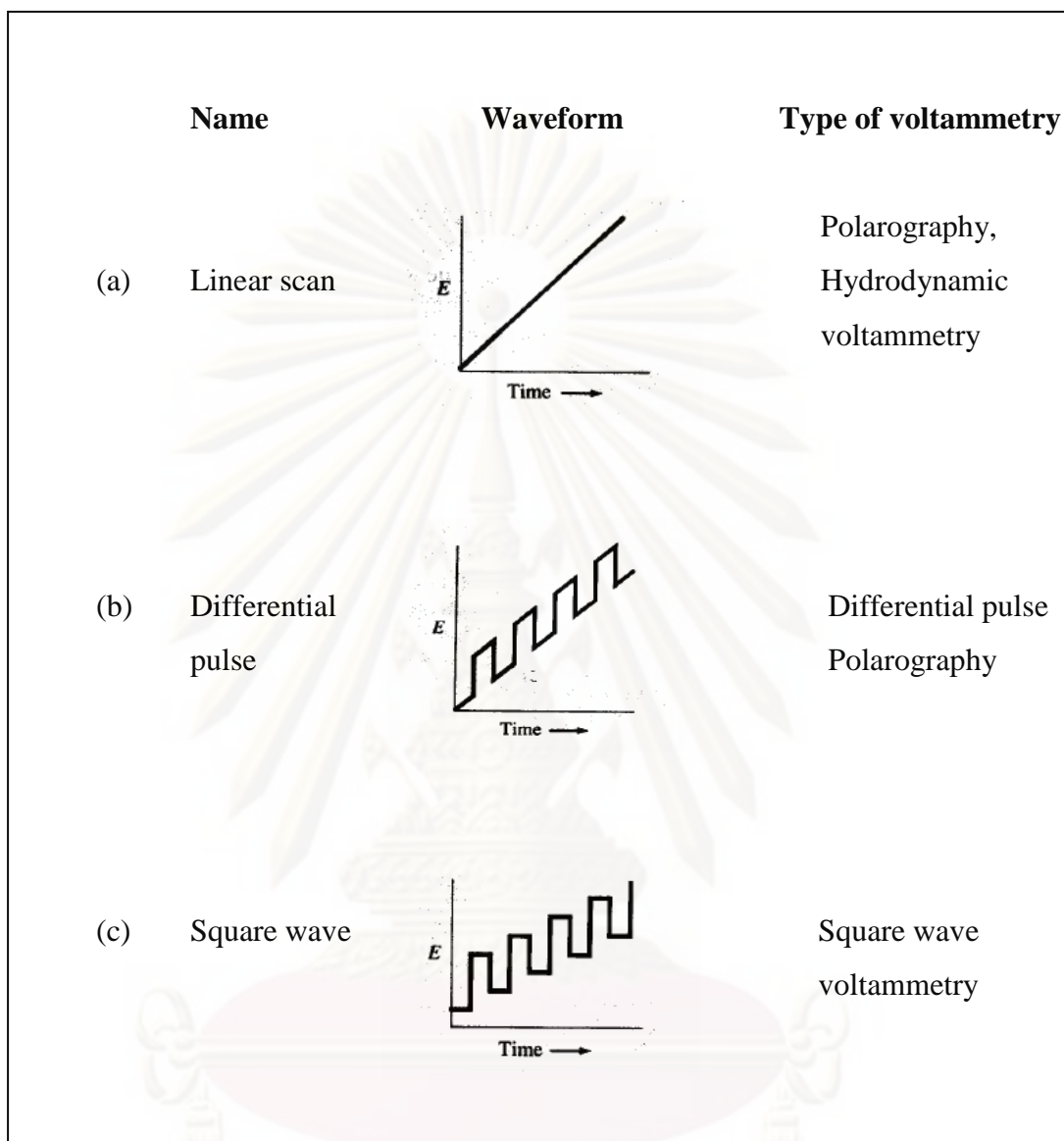
**Figure 2.2** Typical excitation signals for voltammetry

### 2.3.2 Square Wave Voltammetry (SWV)

SWASV uses square wave voltammetry (SWV) at the stripping step of ASV. Discriminating against the charging current, SWV is based on the difference in current decaying rates following a potential step. Shown in Figure 2.3.
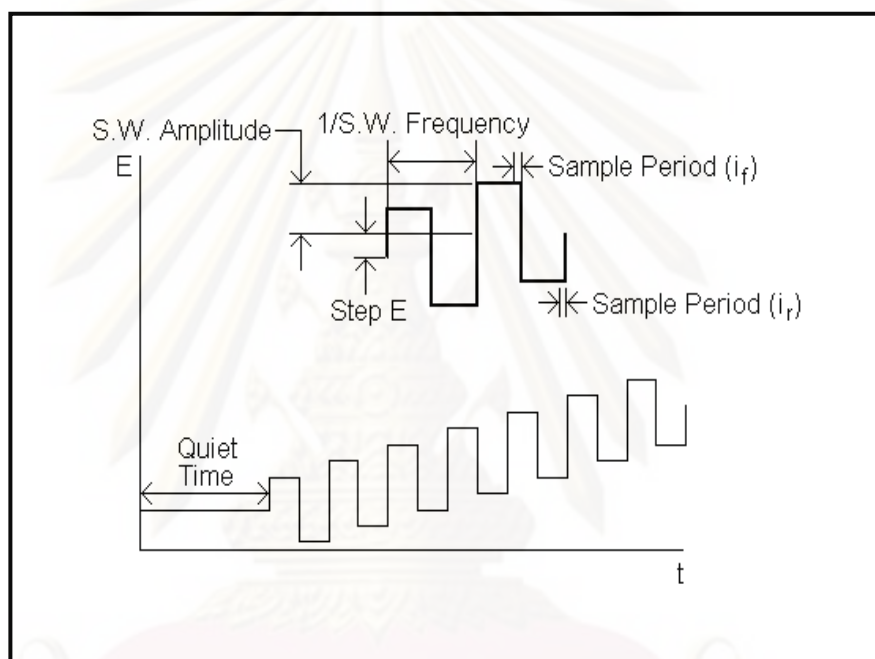


**Figure 2.3**  Square Wave Voltammetry

The square wave potential-time waveform involves the superposition of small square wave potential amplitude on the staircase ramp. By sampling the current just before the square wave changes polarity, the corrected valvue of the changing current is obtained. Moreover, the analytical current is enhanced by combining the opposite current associated with the metal replating.

The sensitivity of this technique can be increased by enhancing the amplitude of the square wave or the frequency. The limits of the enhancing is strictly related to the kinetics aspects of the redox system: it has not to be slower than the velocity of the scanning of potential. The interference due to capacitive current are lowered to minimum because the current is sampled just at the end of the half waves, when the current of the double electrical layer is the least. Detection limits range from 5-50 $\mu g\ L^{-1}$.

### 2.3.3 Stripping Voltammetry (SV)

Stripping voltammetry is an extremely sensitive electrochemical technique for trace metals analysis. The measurement detection limit is down to $10^{-10}$ M.

Stripping voltammetry is a two-step technique. The first step is a deposition step, involves the electrolytic deposition of a small portion of the metal ions in solution into the mercury electrode to preconcentrate the metals. The second step, after the solution is allowed to became quiescent, is the stripping step or the measurement step. In the stripping step, the deposited analytes is redissolved or stripped from the electrode by scanning the potential and the current response of analytes is measured as a function of applied potential. The deposition step is carried out in a stirred solution at a fixed deposition potential ($E_d$) and deposition time ($t_d$). Usually a deposition potential is chosen a few hundred millivolts larger than the polarographic half wave potential of the least easily reduced metal ion to be determind. The optimal deposition time ($t_d$) is adjustable depending on the amount of target elements.

The peak current response depends upon several parameters of the deposition and the stripping steps, as well as on the characteristics of the metal ion and the electrode geometry. For the hanging mercury drop electrode (HMDE), the expression describes the stripping peak current is: $i_p = 2.72 \times 10^5 n^{3/2} A D^{1/2} V^{1/2} C$

Where D  is the diffusion coefficient

V  is the potential scan rate

A  is the electrode area

By using fixed deposition times ($t_d$), the measured voltammetric response (e.g., peak current; ip) was used as parameter for determination of the concentration of analyte.

Different modes of stripping analysis can be employed depending on the nature of the deposition and measurement steps. The stripping techniques employed in this thesis are as follow:

### 2.3.4 Anodic Stripping Voltammetry (ASV)

Anodic stripping voltammetry is a voltammetric method for quantitative determination of specific ionic species. The analyte of interest is electroplated on the working electrode during a deposition step, and oxidized from the electrode during the stripping step. The current is measured during the stripping step. The oxidation of species is registered as a peak in the current signal at the potential at which the species begins to be oxidized. The stripping step can be either linear, staircase, squarewave, or pulse. Anodic stripping voltammetry usually incorporates three electrodes, a working electrode, auxiliary electrode (sometimes called the counter electrode), and reference electrode. The solution being analyzed usually has an electrolyte added to it. For most standard tests, the working electrode is a mercury film electrode. The mercury film forms an amalgam with the analyte of interest, which upon oxidation results in a sharp peak, improving resolution between analytes. The mercury film is formed over a glassy carbon electrode. A mercury drop electrode has also been used for much the same reasons. In cases were the analyte of interest has an oxidizing potential above that of mercury, or where a mercury electrode would be otherwise unsuitable, a solid, inert metal such as silver, gold, or platinum may also be used. Signals for voltammetry as shown in Figure 2.4.
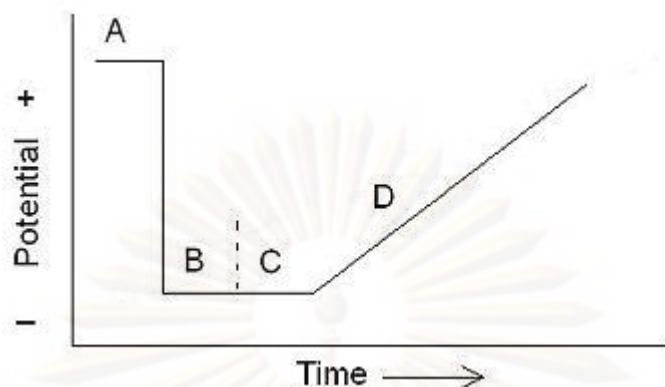
A: Cleaning step,  B: Electroplating step,  C: Equilibration step,  D: Stripping step

**Figure 2.4** Typical excitation signals for voltammetry

Anodic stripping voltammetry is the most widely used form of stripping analysis.  The preconcentration is carried out by cathodic deposition at a controlled time and potential.  After the solution is allowed to become quiescent, the potential is scanned anodically.  During this anodic scan, the re-oxidation of amalgamated metals occurs at specific potential for each species.  The peak currents are obtained for quantitative application.  Redox reactions take place in each step are as follow:

deposition step : $M^{+n} + ne^- \longrightarrow M(Hg)$

measurement (stripping) step : $M(Hg) \longrightarrow M^{+n} + ne^-$

## 2.4  Carbon Nanotube (CNT) [ 26]

### 2.4.1 History of Carbon Nanotubes

Fullerenes are large, closed cage, carbon clusters and have several special properties that were not found in any other compound before.  Therefore, fullerenes in general form an interesting class of compounds that surely will be used in future technologies and applications.  Before the first synthesis and detection of the small fullerenes $C_{60}$ and $C_{70}$, it was generally accepted that these large spherical molecules were unstable.  However, some scientists had already calculated that $C_{60}$ in the gas phase was stable and had a relatively large band gap.  As in the case with numerous, important scientific discoveries, fullerenes were accidentally discovered.  In 1985, Kroto and Smalley found strange results in mass spectra of evaporated carbon samples. Herewith, fullerenes were discovered and their stability in the gas phase was proven.  The search for other fullerenes had started.  Since the discovery in 1991 by Iijima [27] and coworker with adding transition-metal catalysts to the carbon in an arc discharge, carbon nanotubes (CNTs) have been investigated by many researchers over the world.  They can be seen as the nearly one dimensional form of fullerenes. Therefore, these materials are expected to possess additional interesting electronics, mechanic and molecular properties.  Especially in the beginning, all theoretical studies on carbon nanotubes focused on the influence of the nearly one dimensional structure on molecular and electronic properties.

### 2.4.2  Types of Carbon Nanotubes and Related Structures

Carbon nanotubes (CNTs) are hexagonal array of rolled carbon sheets with several microns in length and a few nanometers in diameter [28], which can have a length-to-diameter ratio greater than 1,000.  The bonding in CNTs is sp2, with each carbon atom joined to three neighbours, as in graphite.  The tubes can be considered as rolled up grapheme sheets.  More interestingly, there are three distinct ways that a grapheme sheet can be rolled into a tube.  The structure of CNTs can be specified by chiral vector ($C_h$) which defines how the grapheme sheet is rolled up.  In Figure 2.5,

the integer n and m are the number of unit vectors along two directions in the honeycomb crystal lattice of grapheme, $a_1$ and $a_2$ are the lattice vectors. Chiral vector can be defined by the vector $C_h = na_1 + ma_2$ . If m = 0, the nanotubes are called zigzag. If n = m, the nanotubes are called armchair. Otherwise, they are called chiral. The different chiralities of CNTs are illustrated in Figure 2.6.
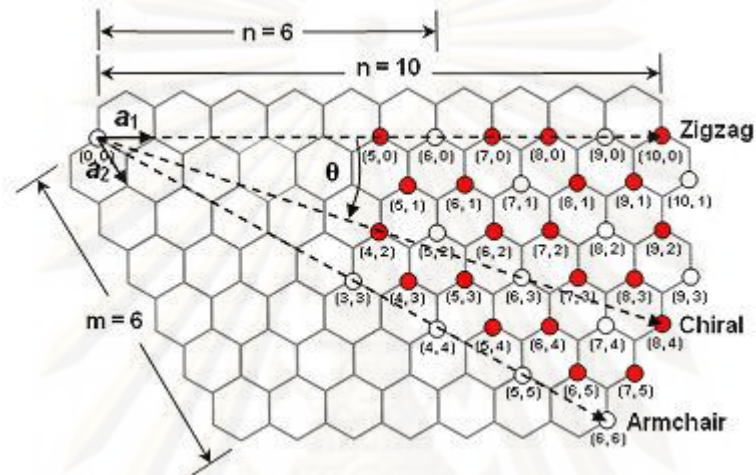


**Figure 2.5** Chiral vector, $C_h$
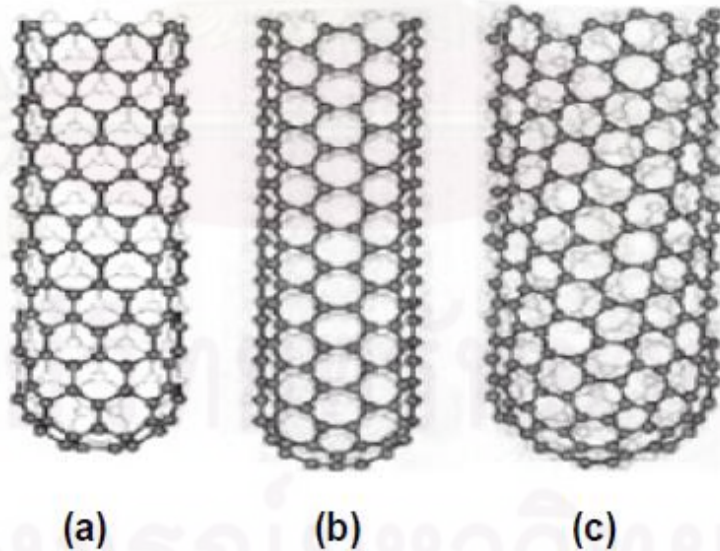


**Figure 2.6** The difference in structure of the tubes (a) Zigzag structure,
(b) Armchair structure and (c) Chiral structure.

More importantly, CNTs can be categorized into two different types:

### 2.4.2.1  Single-Walled Nanotubes

Single-walled nanotubes (SWNTs) is a rolled up tubular shell of grapheme sheet as showed in Figure 2.7.  In addition, SWNTs has a diameter of close to 1 nanometer with a tube length.  The body of the tubular shell is mainly made of hexagonal rings of carbon atoms where as the ends are capped by a dome-shaped half-fullerene molecules.  The natural curvature in the sidewalls is due to the rolling of the sheet into the tubular structure whereas the curvature in the end caps is due to the presence of topological (pentagonal ring) defects in the otherwise hexagonal structure of the underlying lattice.  The role of the pentagonal ring defect is to give a positive curvature to the surface which helps in closing of the tube at the two ends.
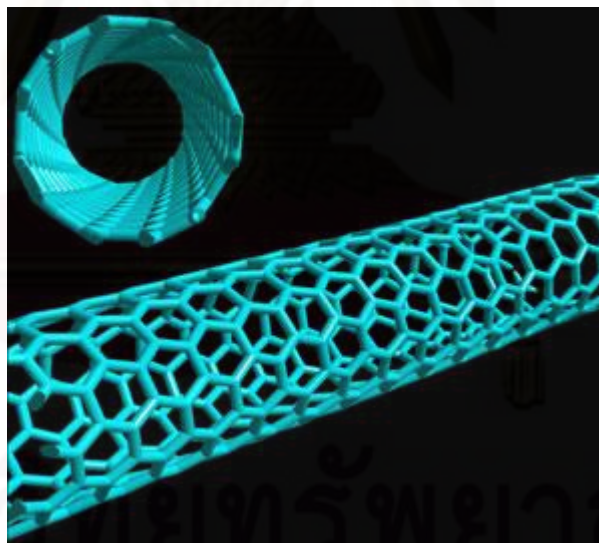


**Figure 2.7**  Single-Walled Nanotubes (SWNTs).

### 2.4.2.2  Multi-Walled Nanotubes

Multi-walled nanotubes (MWNTs), as presented in Figure 2.8, is a rolled up stack of multi grapheme sheets into concentric SWNTs, with the ends again either capped by half-fullerenes of kept open.  The interlayer distance in MWNTs is close to the distance between grapheme layers in graphite, approximately 0.3 nanometers.  Moreover, the length and the diameter of these structures differ a lot from SWNTs
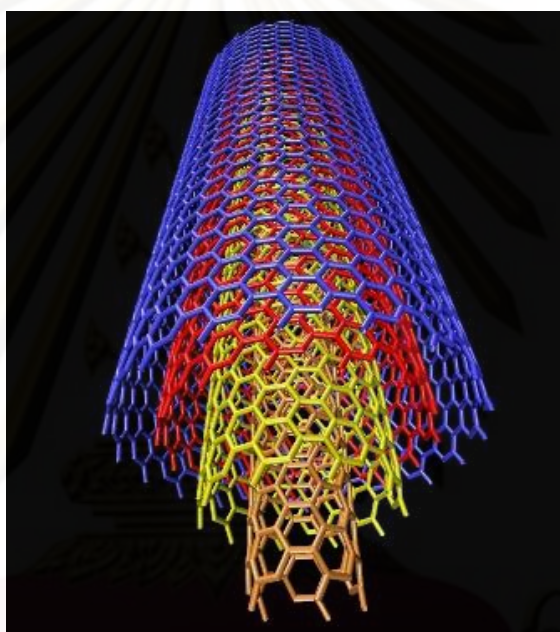


**Figure 2.8**  Multi-Walled Nanotubes (MWNTs).

### 2.4.3  Properties of Carbon Nanotubes [29]

The properties of CNTs are determined to a large extent by their dimensional structure.  The most important properties of CNTs and their molecular background are stated below.

### 2.4.3.1  Chemical Reactivity

The chemical reactivity of CNTs, compared with a grapheme sheet, is enhanced as a direct result of the curvature of CNTs surface.  The reactivity is directly related to the pi-orbital mismatch caused by an increased curvature.  Therefore, a distinction must be made between the sidewall and the end caps of a nanotube.  For the same reason, a smaller nanotube diameter results in increased reactivity.  Covalent chemical modification of either sidewalls or end caps has showed to be possible.  For example, the solubility of CNTs in different solvents can be controlled this way.  However, the study of chemical modifications on nanotube behavior is difficult as the nanotube samples are still not pure enough.

### 2.4.3.2  Electrical Conductivity

Depending on their chiral vector, CNTs with a small diameter are either semiconducting or metallic.  The differences in conducting properties are caused by the molecular structure that results in a different band structure and a band gap.  The differences in conductivity can easily be derived from the grapheme sheet properties.  It was showed that a (n,m) nanotube is metallic as accounts that: $n = m$ or $(n - m) = 3i$, where i is an integer, n and m are defining the nanotube.  Moreover, the conductivity of CNTs is determined by quantum mechanical aspects and proved to be independence from the nanotube length.

### 2.4.3.3  Thermal Conductivity and Resistance

All nanotubes are the excellent good thermal conductors along the tube, exhibiting a property known as ballistic conduction but good insulators laterally to the tube axis.  CNTs are able to transmit up to 6,000 W/m/K at room temperature; compare this to copper, a metal well known for its good thermal conductivity, which only transmits 385 W/m/K.  The temperature stability of carbon nanotubes is estimated to be up to 2,800 degrees Celsius in vacuum and about 750 degree Celsius in air.

### 2.4.3.4  Mechanical Strength

CNTs are one of the strong materials known in terms of tensile strength as listed in Table 2.4.  This strength results from the covalent $sp^2$ bonds formed between the individual carbon atoms.  Besides, CNTs have a very large Young's modulus in their axial direction.  The nanotube as a whole is very flexible because of the great length.  Therefore, these compounds are potentially suitable for applications in composite materials that need anisotropic properties.  However, CNTs are not nearly as strong under compression.  Because of their hollow structure and high aspect ratio, they tend to undergo when placed under compressive, torsional or bending stress.

**Table 2.4** Young's modulus, tensile strength and density of carbon nanotubes compared with other materials.

| Materials | Young's Modulus (GPa) | Tensile Strength (GPa) | Density (g/cm$^3$) |
|---|---|---|---|
| Single-walled nanotubes | 1,054 | 150 | - |
| Multi-walled nanotubes | 1,200 | 150 | 2.6 |
| Steel | 208 | 0.4 | 7.8 |
| Epoxy | 3.5 | 0.005 | 1.25 |
| Wood | 16 | 0.008 | 0.6 |

## 2.5 Screen-printed Carbon (SPC) [ 30]

Screen-printing technology is a technique often used in the fabrication of electrodes for the development of disposable electrochemical biosensors [30]. A screen printed electrode is a planar device based on multiple layers of a graphite-powder-based ink printed on a polyimide, plastic, epoxy or alumina ceramic substrates. Graphite's structure is shown in Figure 2.9 . The advantages of designable techniques, adapted from microelectronics, have made screen-printing technology one of the most important technique for fabrication of single-use biosensors in the market of handheld instruments. The main advantages of the screen printed electrode include simplicity, versatility, modest cost, portability, ease of operation, reliability, small size, and mass production capabilities, which lead to its development in various applications in the electroanalytical field.
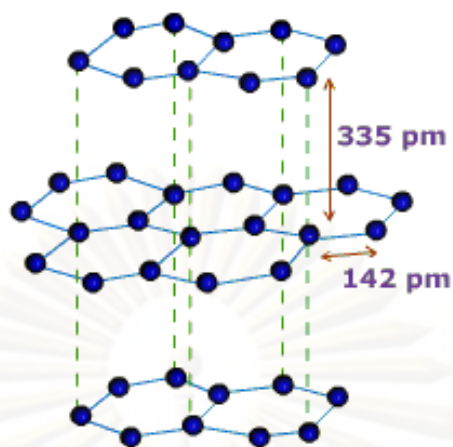
**Figure 2.9**  Crystal structure of graphite showing unit cell

## 2.6  Flow-Analysis Techniques

Flow-based methods are well established and widely used as automated methods for analysis.  In this section two flow-based methods, flow injection analysis and sequential injection analysis, are described.

### 2.6.1  Flow Injection Analysis [31]

Flow injection analysis (FIA) is a well-established continuous-flow technique that has proven its utility in both basic research and applications.  This technique was initiated almost simultaneously by Ruzicka and Hansen [32] in Denmark and Stewart and coworkers [33] in the United states in the mid 1970s.  The principle of this technique is to exploit controlled dispersion in narrow bore tubing, sometimes under the name of "zone fluidics".  A typical FIA manifold is illustrated in Figure 2.10.  A volume of sample is inserted into the sample loop of an injection valve  while a stream of carrier and a stream of reagent are mixed at a confluence point and are flowing constantly through the detector.  After the sample loop is filled with the sample, the valve is rotated so that the sample is injected into the flowing carrier stream and physically transported by the carrier to the confluence point where it mixes with the reagent.  In the course of its travel through the reaction coil, the sample zone disperses and reacts with the reagent to form a detectable species.

The detectable species gives rise to a transient peak when it passes through the flow-cell of the detector.
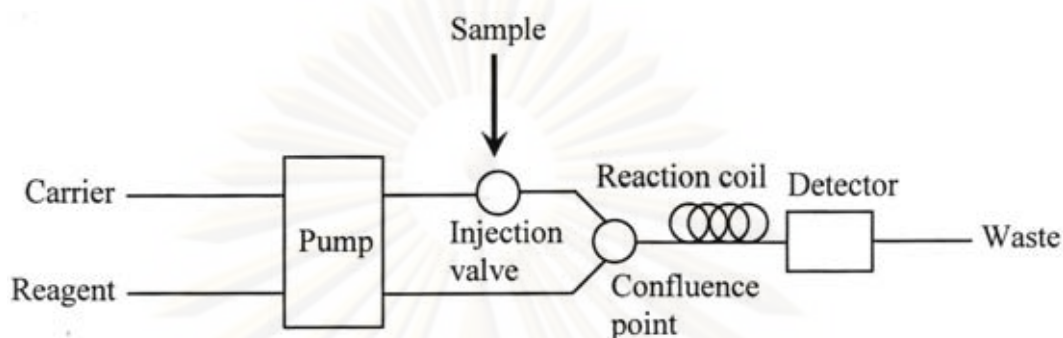


**Figure 2.10** A typical manifold of flow injection analysis.

### 2.6.2 Sequential Injection Analysis [31,34,35]

Sequential injection analysis (SIA) was first proposed by Ruzicka and Marshall [36] in 1990 as a possible alternative to FIA. The principles upon which SIA is based are similar to those of FIA, namely controlled partial dispersion and reproducible sample handling. In contrast to FIA, SIA employs the computer-controlled multi-position selection valve and bi-directional pump operated synchronously. A typical SIA manifold is illustrated in Figure 2.11.
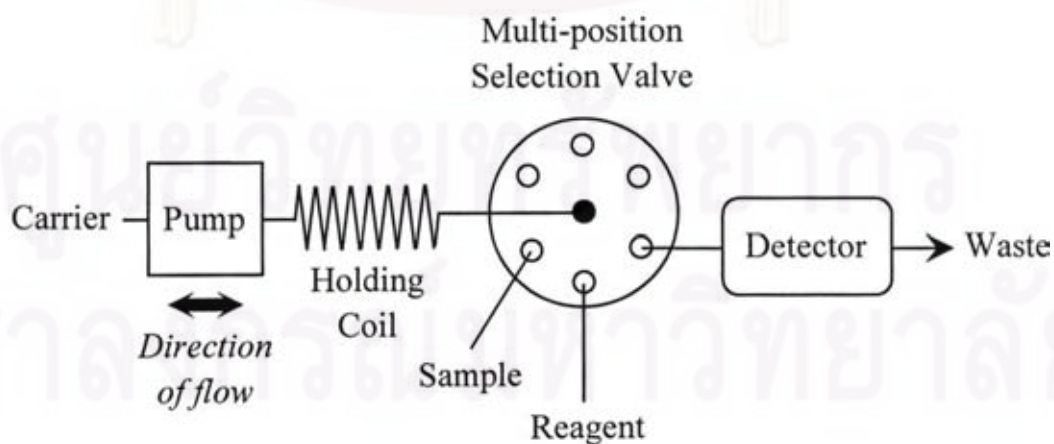


**Figure 2.11** A typical manifold of sequential injection analysis.

Propulsion of solution through the manifold tubing (typically 0.5-0.8 mm i.d. PTFE) is achieved using a peristaltic pump or a syringe pump. A holding coil is placed between the pump and the common port of the multi-position selection valve. The selection ports of the valve are coupled to sample and reagent reservoirs as well as a detector. The valve is directed to a selection port that is connected to the sample line and a zone of the sample is drawn up into the holding coil by the pump. Then, the selection valve is directed to a port that is connected to a reagent line and a zone of the reagent is drawn up into the holding coil adjacent to the sample zone. Then, the selection valve is switched to a port that is connected to a detector. As the zone move towards the detector, zone dispersion and overlap occurs, resulting in the formation of the detectable species that is monitored by the detector. The vast majority of SIA procedures are still based on the solution-phase chemistry described above.

Comparing SIA and FIA for this simple sample manipulation, the following points can be made in Table 2.5.

**Table 2.5** Comparison between SIA and FIA

| SIA | FIA |
|---|---|
| A simpler, more robust single channel manifold even with multi-component chemical systems. | Simplicity and low cost instrumentation |
| Syringe pumps offer increased robustness with precise operation and little maintenance for process applications. | Multi-channel peristaltic pumps |
| Sample and reagent consumptions are minimized due to the discontinuous operation mode. | High sampling rate |
| Selection valve provides a means for performing convenient automated calibration. | Reduced analyses cost when a lot of samples have to be analyzed |

| SIA | FIA |
|---|---|
| Accurate handling of sample and reagent zones necessitates computer control, so automation becomes essential. | Automation in sample preparation and detection |

In recent years, it has become apparent that the scope of SIA can be extended to encompass a variety of more complex, on-line, sample-manipulation and pretreatment procedures. Then, the ports of the multi-position selection valve are coupled to various units (e.g., reservoirs, detectors, pumps, reactors, separators, special cells, and other manifolds), as illustrated in Figure 2.12 [37]. After aspiration of the sample zone into the holding coil via the sample line, the sample can be manipulated in different ways within the SIA manifold by taking advantage of the stopped-flow, bi-directional nature of fluid handling in SIA.
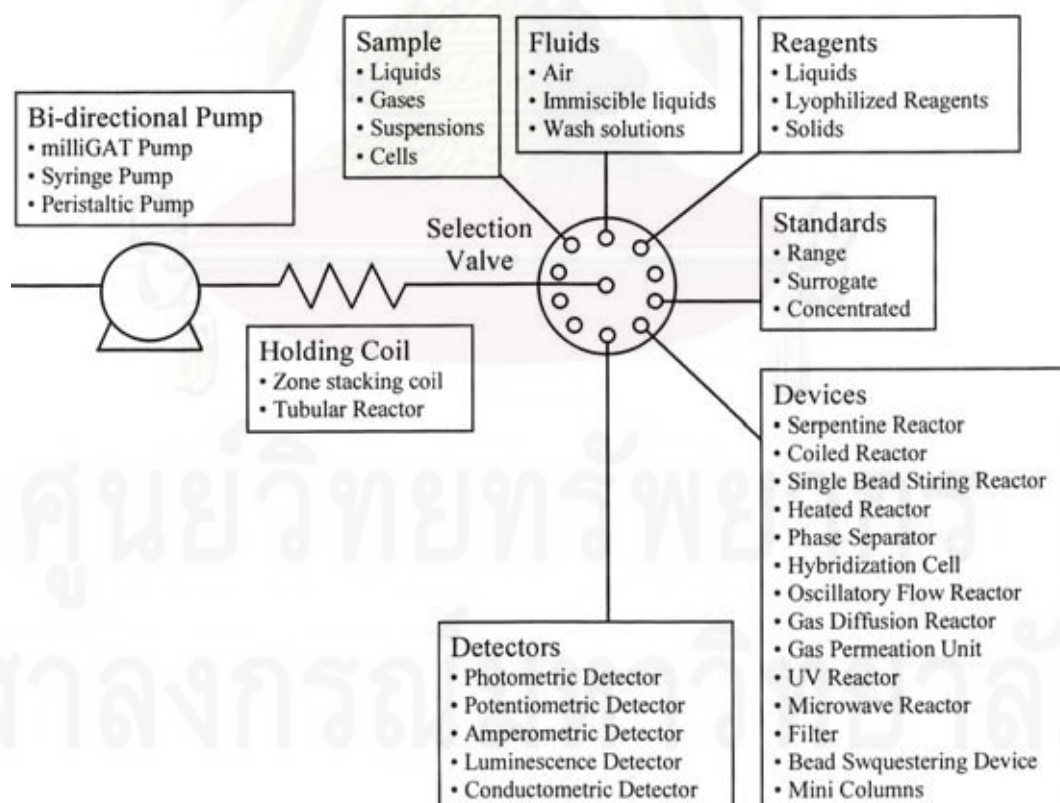


**Figure 2.12** Potential of SIA for automated sample pre-treatment.

# CHAPTER III

# EXPERIMENTAL

## 3.1   Instruments and Apparatus

The employed electrochemical instruments and apparatus are summarized in Table 3.1.

**Table 3.1** Electrochemical instruments

| Instrument | Company (Country) |
|---|---|
| 1.   potentiostat/galvanostat PG-30 | Metrohm (Switzerland) |
| 2.   working electrode | |
| 2.1  bismuth film screen-printed carbon electrodes (Bi-SPCEs) | - |
| 2.2  bismuth film screen-printed carbon nanotubes electrodes (Bi-SPCNTEs) | (China) |
| 3.   reference electrode | |
| 3.1  silver/silver chloride (Ag/AgCl) electrode | (Japan) |
| 4.   counter electrode | |
| 4.1  stainless-steel tube (Pt) | Bioanalytical System Inc. (USA) |

| Instrument | Company (Country) |
|---|---|
| 5.   sequential injection analysis system | (Japan) |
| 6.   LabVIEW® software  Ver 7.1 | - |
| 7.   other apparatus | |
| 7.1 electrochemical flow cell | Bioanalytical System Inc. (USA) |
| 7.2 teflon cell gasket | Bioanalytical System Inc. (USA) |
| 7.3 milli Q water system, R ≥ 18.2 MΩ cm | Millipore (USA) |
| 7.4 faraday cage | - |
| 7.5 PTFE tubing | Bioanalytical System Inc. (USA) |
| 7.6 analytical balance (Mettler AT 200) | Metrohm (Switzerland) |
| 7.7 ultrasonic bath (ULTRAsonik 28H) | ESP Chemicals, Inc. (USA) |
| 7.8 autopipette and tips | Eppendorf (Germany) |
| 7.9 filters membrane (0.2 μM, 47 mm) | Whatman |

## 3.2 Chemicals

All chemicals employed in this research are Analytical Reagent (AR) grade. Milli-Q water was used for preparing all chemical solutions. Chemicals and their suppliers are summarized in Table 3.2.

**Table 3.2** Chemicals

| Chemical | Manufacturer (Country) |
|---|---|
| 1. carbon nanotube 99%, CNT | Chang Mai University (Thailand) |
| 2. hydrochloric acid, fuming 37%, HCl | Merck (Germany) |
| 3. nitric acid 65%, $HNO_3$ | Merck (Germany) |
| 4. sulfuric acid 95-97%, $H_2SO_4$ | Merck (Germany) |
| 5. zinc (II) nitrate, standard solution 1000 ppm | BDH Chemicals (UK) |
| 6. cadmium (II) nitrate, standard solution 1000 ppm | BDH Chemicals (UK) |
| 7. lead (II) nitrate, standard solution 1000 ppm | BDH Chemicals (UK) |
| 8. bismuth (III) standard solution 1000 ppm | Wako Pure Chemical Industries (Japan) |
| 9. 2-butylglycolacetate 99% | Sigma-Aldrich (USA) |
| 10. diethelene glycol monobutyl ether | Fluka (UK) |
| 11. acetone | Merck (Germany) |

## 3.3 Preparation of Reagents

The following section explains procedures for preparing chemical solutions in this work.

### 3.3.1. Standard Lead (II), Cadmium (II) and Zinc (II) Solution

A 10 mg $L^{-1}$ standard solution of Pb (II), Cd (II) and Zn (II) was prepared by diluting 100 µL each of 1000 mg $L^{-1}$ Pb, Cd and Zn atomic absorption analysis standard solution (ultrapure grade, Chemical , England) to 10 mL with 1.0 M hydrochloric acid solution.

The working standard solutions of Pb (II), Cd (II) and Zn (II) were daily prepared by appropriate dilution of the intermediate standard solution with 1 M hydrochloric acid solution.

### 3.3.2 Hydrochloric Acid Solution

A 1 M hydrochloric acid solution was prepared by diluting 83.60 mL of concentrated hydrochloric acid (electronic grade, 37% w/w, 1.18 g $mL^{-1}$, Merck Chemicals, Germany) to 1000 mL with ultrapure water.

### 3.3.3 Bismuth (III) Plating Solution

A 10 mg $L^{-1}$ stock solution of Bi (III) was prepared by diluting 100 µL of 1000 mg $L^{-1}$ Bi atomic absorption analysis standard solution (Wako Pure Chemical Industries, Ltd., Japan) to 10 mL with 1.0 M hydrochloric acid solution.

A Bi (III) plating solution was prepared by appropriate dilution of the stock solution of Bi(III) with 1 M hydrochloric acid.

## 3.4    Experimental Procedures

In this section, it mainly consists of procedures for CNT modification, electrode preparation, measurement procedure and sample preparation

### 3.4.1    Modification of Carbon Nanotubes (CNTs) [38]

In order to functionalize CNT with active groups such as carboxylic acid, 1.0 g of CNTs was dispersed in 50 mL of 3:2 v/v mixed concentrated $HNO_3$ and $H_2SO_4$ and then the mixture was agitated by ultrasonic wave for 12 h.  After that, CNTs mixture was washed with Milli-Q water until pH of the mixture approached 7. Finally, the mixture was filtered and dried at 80°C **[38]**.  The information of functional groups attached on modified CNT was provided by Fourier transform infrared (FTIR) spectrometer.

### 3.4.2    Electrode Preparation

#### 3.4.2.1    Screen-printed Carbon Electrodes (SPCEs)

The electrodes  were  screen-printed  in house using carbon ink (Electrodag PF-407C,  Acheson,  USA),  silver ink (Electrodag 7019,  Acheson, USA) and ceramic substrates.  Bismuth film screen-printed carbon electrodes (Bi-SPCEs) were prepared by on-line in situ plating.

#### 3.4.2.2    Screen-printed Carbon Nanotubes Electrodes (SPCNTEs)

The electrodes were screen-printed in house using multi-walled carbon nanotubes (MWCNTs) mixed with carbon ink (Electrodag PF-407C, Acheson, USA), silver ink (Electrodag 7019, Acheson,  USA) and ceramic substrates. Bismuth film screen-printed carbon electrodes (Bi-SPCEs) were prepared by on-line in situ plating.

### 3.4.3 Measurement Procedure

A sequential injection system for determination of lead (II), cadmium (II) and zinc (II) by square wave anodic stripping voltammetry, as shown in Figure 3.1, consist of 3-way syringe pump (Hamilton, USA) and a 8-port selection valve (Hamilton, USA). PTFE tubing was used for flow lines (0.5 mm i.d.) and a holding coil (1.5 mm i.d.). The system was computer controlled by using a program written by LabVIEW® software Ver. 7.1 (National Instrument).
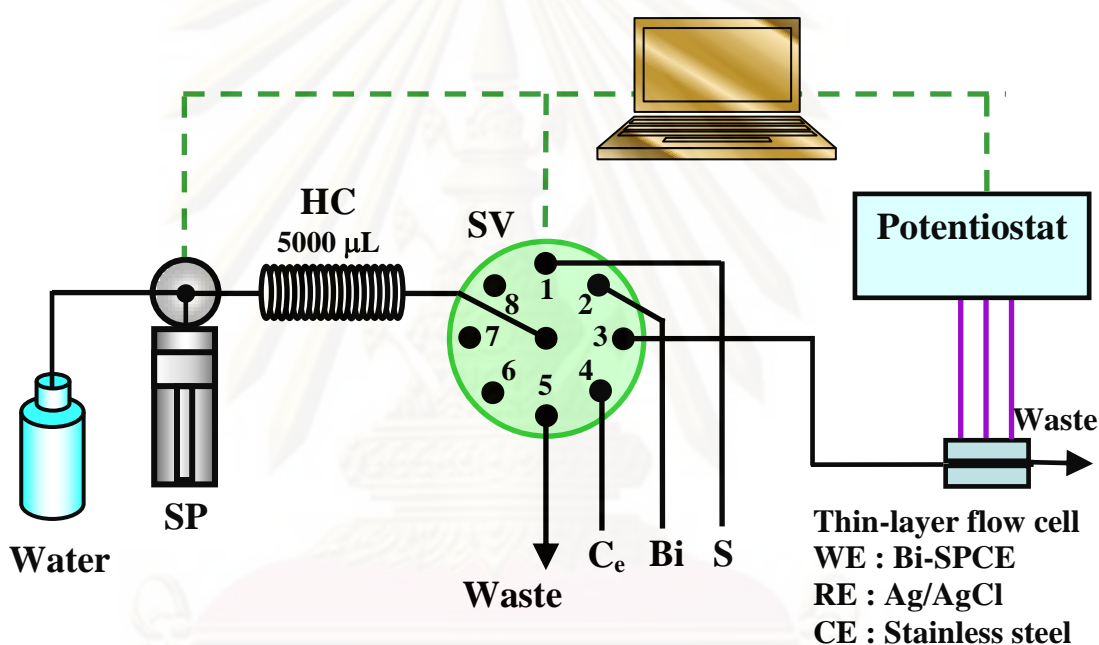


**Figure 3.1** Schematic diagram of SIA-SWASV for determination of lead (II),
cadmium (II) and zinc (II). SP: syringe pump; SV: selection valve;
HC: holding coil; Ce: electrode cleaning solution ( 1M HCl),
Bi: Bismuth (III) plating solution, S: sample solution;
WE: working electrode; RE: reference electrode; CE: counter electrode.

Electrochemical measurements were carried out in a thin-layer flow cell (Bioanalytical Systems, USA) using PGSTAT 30 instrument (Eco Chemie B.V., The Netherlands). The thin-layer flow cell consisted of a gasket as a spacer, a bismuth film screen-printed carbon nanotube electrode (Bi-SPCNT) as a working electrode, a Ag/AgCl electrode (3 M KCl) as a reference electrode, and a stainless steel tube as a counter electrode and a solution outlet of the flow cell. The experiments were carried out in a Faraday cage to reduce electrical noise.

Step sequence for determination of metals by sequential injection-square wave anodic stripping voltammetry (SIA-SWASV) are shown in Table 3.3.

**Table 3.3** Step sequence for the determination of heavy metals by SIA-SWASV.

| Step | Valve position (SV) | Volume (μL) | Flow rate (μL s$^{-1}$) | Duration (s) | Electrode potential (V) | Description |
|------|------|------|------|------|------|------|
| 1 | 1 | 1440 | 200 | 7.2 | +0.5[a] | Aspirate sample solution into HC |
| 2 | 2 | 720 | 200 | 3.6 | +0.5[a] | Aspirate Bi(III) solution into HC |
| 3 | 3 | 2160 | 12 | 180 | -1.4 | Dispense Bi(III) solution and sample solution into flow cell for in situ plating of Bi and deposition of heavy metals |
| 4 | 3 | - | 0 | 10 | -1.4 | Equilibration |
| 5 | 3 | - | 0 | 10 | Scan (-1.3 to 0) | Stripping and recording of voltammogram |
| 6 | 4 | 1200 | 200 | 6 | +0.3 | Aspirate 1 M HCl into HC |
| 7 | 3 | 1200 | 50 | 24 | +0.3 | Dispense 1 M HCl into flow cell for electrode cleaning |

[a] Conditioning potential

Zones of the sample and the Bi (III) plating solution were sequentially aspirated into the holding coil (Steps 1 and 2). Then, sample and Bi (III) plating solution were flowed directly to the flow cell while the potential of the electrode was maintained at -1.4 V vs. Ag/AgCl for 180 s as the preconcentration step (Step 3). After 10 s of equilibration (Step 4), square-wave voltammograms with a frequency of 50 Hz, a step potential of 5 mV, and a pulse amplitude of 50 mV were recorded from -1.4 to 0 V vs. Ag/AgCl (Step 5). Finally, the electrode was cleaned to remove any remaining analyte metals and bismuth film at +0.3 V vs. Ag/AgCl in flowing supporting electrolyte for 30 s (Steps 6 and 7). A measurement cycle for three analytes including Pb (II), Cd (II), and Zn (II) is about 4 min. The electrode was then ready for a new stripping cycle. 1 M hydrochloric acid was used as a supporting electrolyte for all steps. All experiments were performed at room temperature (25 °C) without removing oxygen from the solution.

### 3.4.4   Sample Preparation

The samples are *A. paniculata* from leaves (obtained from south of Thailand). Samples were digested with the mixtures of concentrated nitric ($HNO_3$) and perchloric ($HClO_4$) acid solution. Concentrated $HNO_3$ and $HClO_4$ acid solution in the ratios of 1:0, 4:1, 3:2, 1:1, 2:3, 1:4 and 0:1 (v:v) were evaluated for sample digestion [21]. The dried samples were spiked with the different concentrations of metal standard solution (20, 30, 40, 50, and 60 ppb of Pb (II), Cd (II), and Zn (II) in order to check the performance of extraction method by calculation of the % recovery from the standard addition samples, samples were heated up at 100 °C for 4 h to digest samples and evaporate solvent. Then, 5 mL of 1 M HCl was added and heated until a clear solution was formed (~1 h) before introducing into the SIA-ASV system.

# CHAPTER IV

# RESULTS AND DISCUSSION

This chapter describes experimental results related to the modification of Carbon Nanotube (CNT). Comparison of the electrochemical response between Bi-SPCNTEs and Bi-SPCEs. Optimization of operation conditions such as percentages of CNTs to carbon ink, effect of bismuth plating solution concentration, effect of deposition time and effect of flow rate, analytical performance of the Bi-SPCNTE and analytical applications.

## 4.1    Modification of Carbon Nanotubes (CNTs)

After CNT was functionalized with carboxylic acid groups, fourier transform infrared (FTIR) spectroscopy was introduced to obtain the information about the functional groups attached on the modified CNT, in comparison with the unmodified CNT.

Since the surface of raw CNT is chemically inert and hydrophobic, CNT is unfavorable for supporting catalyst. Therefore, the modification of CNT surface with functional groups is essential. FTIR spectra of unmodified and modified CNT are presented in Figure 4.1. In both cases, the peak at about 3,400 $cm^{-1}$ can be attributed to OH symmetrical stretching whereas the peak at about 1,630 $cm^{-1}$ is suggested to be C=C stretching [39]. For the unmodified CNT (Fig. 4.1a), the peak at 1,130 $cm^{-1}$ can be attributed to C–H bending. After CNT modification with the acid treatment, FTIR spectrum of the modified CNT (Fig. 4.1b) shows the peaks at 1,550 and 1,720 $cm^{-1}$ representing $COO^-$ and C=O stretching of carboxyl group as well as the peak at 1,200 $cm^{-1}$ corresponding to C–O stretching [38,40]. FTIR result revealed that oxygen-containing functional groups can be introduced to CNT by the oxidative treatment with mixed strong acids, making CNT favor high loading of well-dispersed metal nanoparticles.
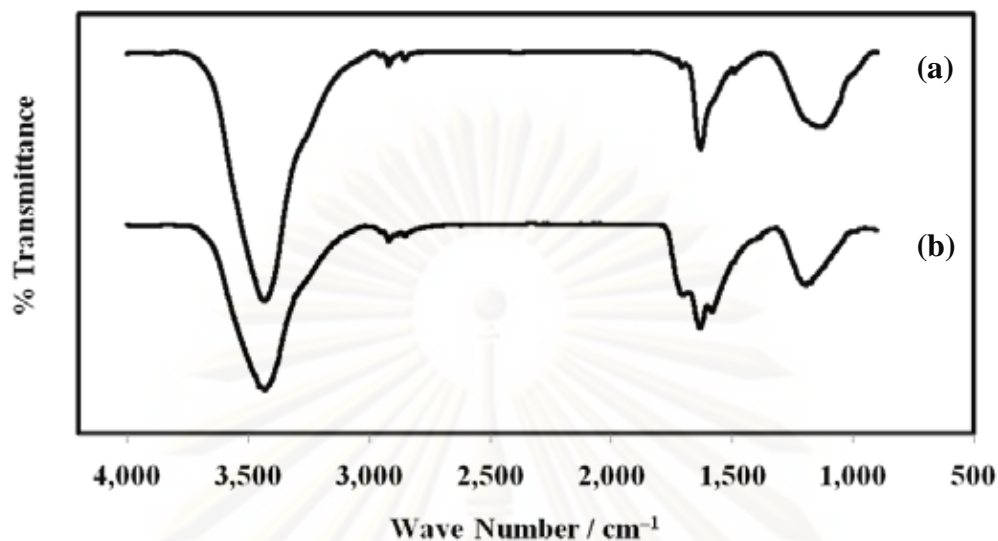
**Figure 4.1** FTIR spectra of (a) unmodified and (b) modified CNT.

## 4.2 Comparison of the Electrochemical Response between Bi-SPCNTEs and Bi-SPCEs

The background current was enlarged about 5-10 times in SPCNTE compared to SPCE.  Only CNTs electrodes produced a relatively high background current due to their high surface area [16,17].  However, the electrochemical signal for heavy metals on the Bi-modified CNTs electrode also depended on the property of bismuth film on that substrate.  Anodic stripping peak currents of Pb (II), Cd (II), and Zn (II) on Bi-SPCNTEs and Bi-SPCEs are compared in Figure 4.2 .

**Figure 4.2** Comparison of peak height current of 50 µg L$^{-1}$ for Pb (II) and Cd (II)
and 100 µg L$^{-1}$ Zn (II) on Bi-SPCEs and Bi-SPCNTEs
(2% of CNTs:carbon ink,w/w) with -1.4 V of deposition potential
for 180 s and 12 µL s$^{-1}$ flow rate .

The results indicated that anodic stripping peak currents of heavy metals on Bi-SPCNTE (2% CNTs) were higher, compared with those of the Bi-SPCE using the same concentration at 200 µg $L^{-1}$ of Bi(III) plating solution. The improved electroanalytical performance of Bi-SPCNTE is probably due to different surface nature/structure and related characteristics of the substrate electrode. When using CNTs screen-printed electrode as substrate electrode for the in situ plating of bismuth films, the real active electrode surface at the given overall area is larger than the one at carbon electrode. In addition, it may relate to the high adsorptive ability and larger quantities of active sites on CNTs surface [16,17].

## 4.3    Optimization of Operation Conditions

### 4.3.1    Percentages of CNTs to Carbon Ink

SPCNTEs were prepared from the mixtures of CNT and carbon ink. Even though CNTs have been proven to possess potential for heavy metals analysis due to their high electrical conductivity and high surface area, they generate a higher background current than unmodified carbon electrodes. In order to obtain the electrochemical signal for heavy metals detection with the highest signal-to-noise ratio, the percentages of CNTs to carbon ink with 5%, 10% and 15% (w/w) were studied by SIA-ASV. Anodic stripping voltammograms of 50 µg$L^{-1}$ Pb (II) and Cd (II), and 100 µg $L^{-1}$ Zn (II) on Bi-SPCNTEs at the different percentages of CNT are shown in Figure 4.3.

**Figure 4.3** Comparison of peak height current of 50 µg L$^{-1}$ for Pb (II) and Cd (II) and 100 µg L$^{-1}$ Zn (II) on Bi-SPCNTEs at 5%, 10%, and 15% (w/w) of CNTs: carbon ink. Experimental conditions; -1.4 V of deposition potential for 180 s and 12 µL s$^{-1}$ flow rate.

It was clear that anodic stripping peak current of Pb (II), Cd (II), and Zn (II) decreased with increasing percentage of CNTs. Owing to increase the electrode surface area of the CNTs could be attributed to the larger background current [41-43]. Therefore, this work selected the best percentage of CNTs 5% (w/w) for the next experiment.

### 4.3.2 Effect of Bismuth Plating Solution Concentration

In this work, bismuth film was produced on SPCEs and SPCNTEs by on-line in situ plating between each run. Bi (III) plating solution was aspirated into the flow system followed by aspiration of sample solution into the holding coil. Next, both solution zones were delivered to flow cell so that the Bi was deposited first, followed by the heavy metals in the sample. At the end of each analytical cycle, the bismuth film was stripped off by holding the potential of the working electrode at +0.3 V for 30 s. The most critical parameter in this step is the thickness of the bismuth film which depends on the aspirated volume and the concentration of the bismuth plating solution [9,14,15]. Here, the thickness of the bismuth film was optimized by varying the concentration of the Bi (III) plating solution in the range of 10-300 $\mu$g L$^{-1}$ whereas the volume of the bismuth solution was held constantly. The results are shown in Figure 4.4 .
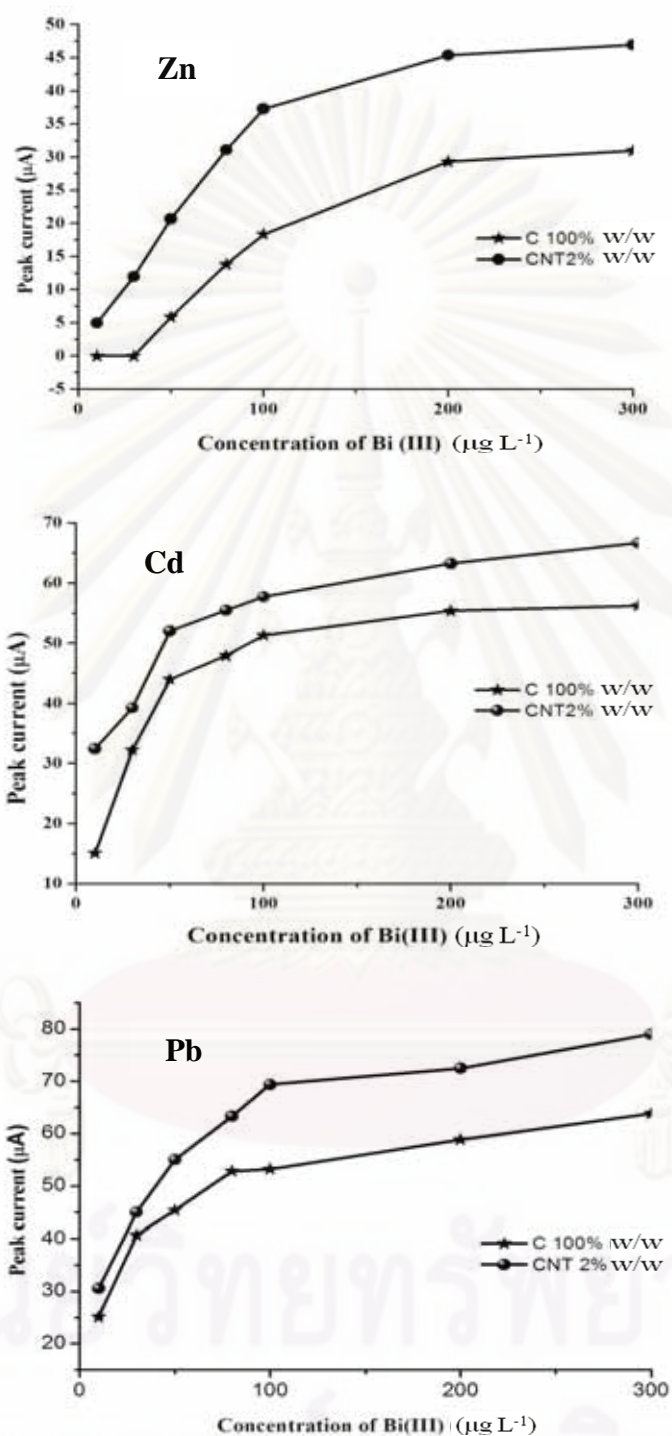
**Figure 4.4** Comparison of peak height current of 50 µg L$^{-1}$ for Pb (II) and Cd (II)
and 100 µg L$^{-1}$ Zn (II) on Bi-SPCNTEs at 10, 50, 100, 150, 200, 250,
and 300 µg L$^{-1}$ of Bi (III) plating solution. Experimental conditions;
-1.4 V of deposition potential for 180 s and 12 µL s$^{-1}$ flow rate .

The anodic stripping peak currents of 50 µg L$^{-1}$ for Pb (II) and Cd (II) were increased up to 100 µg L$^{-1}$ of Bi (III) plating solution concentration and 200 µg L$^{-1}$ for Zn (II). After that, the signals remained constantly for Pb (II) and Cd (II) and slightly decreased for Zn (II) when increasing Bi (III) concentration. The results are shown that the Bi (III) concentration of 150 µg L$^{-1}$ enough to detected three heavy metals, then it was chosen for the simultaneous determinations of Pb (II), Cd (II) and Zn (II) .

### 4.3.3 Effect of Deposition Time

The effect of the deposition time on the anodic stripping peak currents of Pb (II), Cd (II), and Zn (II) was studied in the range of 60-300 s. The plots of the anodic stripping peak currents of three heavy metals as a function of deposition time are shown in Figure 4.5.
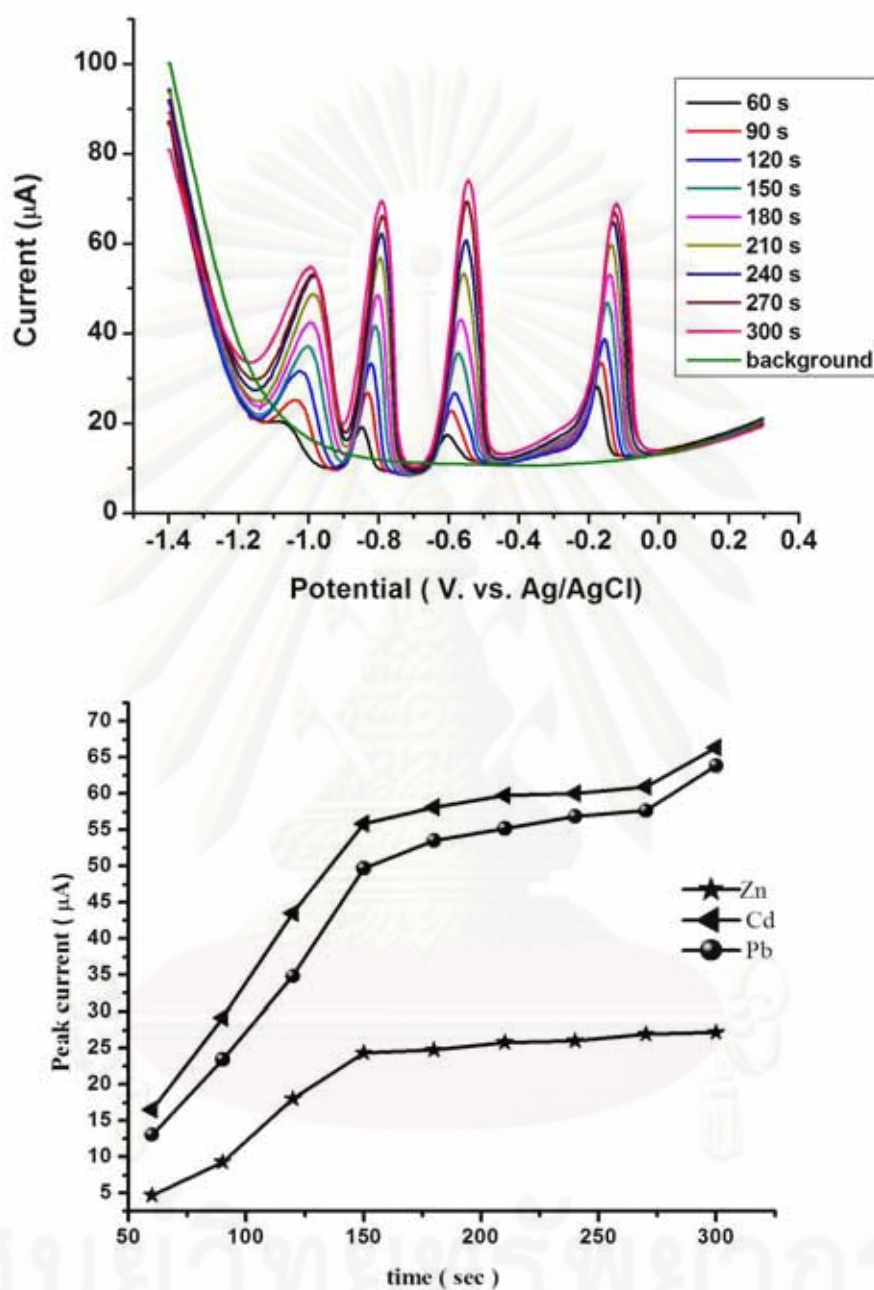
**Figure 4.5** Comparison of peak height current of 50 µg L$^{-1}$ for Pb (II) and Cd (II)
and 100 µg L$^{-1}$ Zn (II) on Bi-SPCNTEs at 150 µg L$^{-1}$ of Bi (III) plating
solution at different deposition times ( 60, 90, 120, 150, 180, 210, 240,
270 and 300 s).  Experimental conditions;   -1.4 V of deposition
potential and 12 µL s$^{-1}$ flow rate .

The results indicated that the stripping peak currents of three heavy metals increased with increasing the deposition time. However, the peak currents slightly increased for Zn (II) after 180 s. Thus, a deposition time of 180 s was chosen to compromise between the sensitivity and analysis time.

### 4.3.4 Effect of Flow Rate

The flow rate plays an important role in the sensitivity and analysis time of metal analysis. Hence, the influence of the flow rate on the stripping peak currents was investigated in the range of 4-18 µL s$^{-1}$. Deposition time of 180 s was fixed and the ratio between the metal ion solution and Bi (III) plating solution was set at 2:1. The stripping peak currents rapidly increased when the flow rate increased in the range of 4-16 µL s$^{-1}$ for Pb (II) and Cd (II) and 4-12 µL s$^{-1}$ for Zn (II) as shown in Figure 4.6.

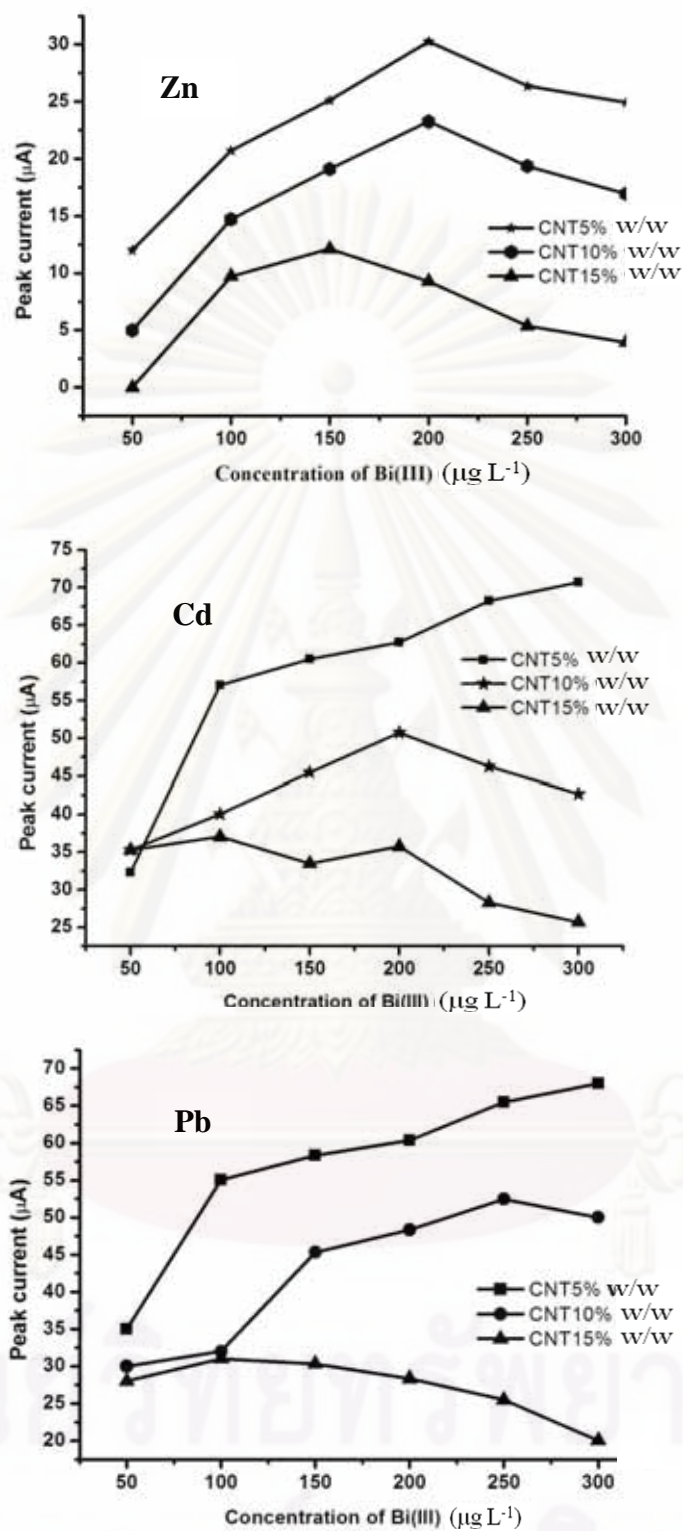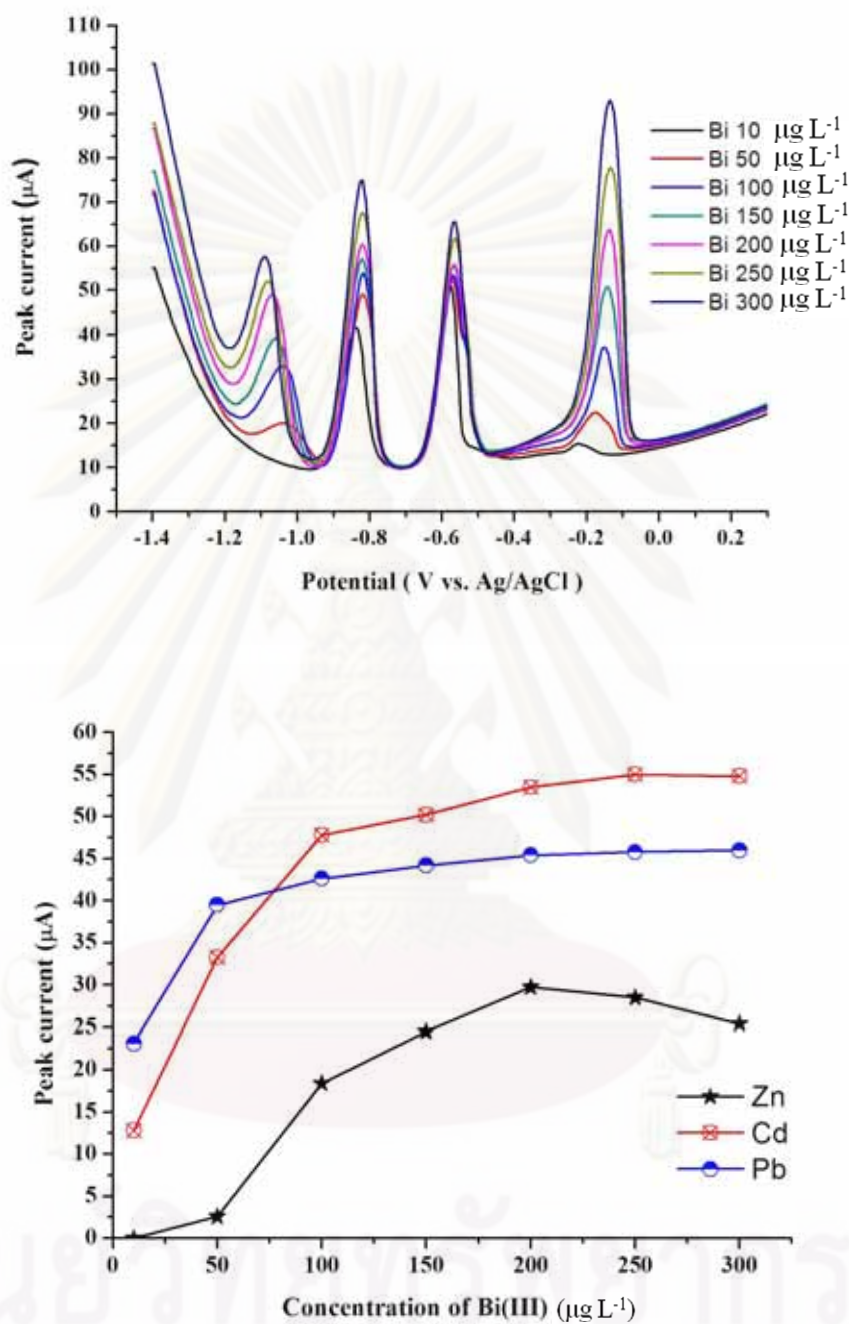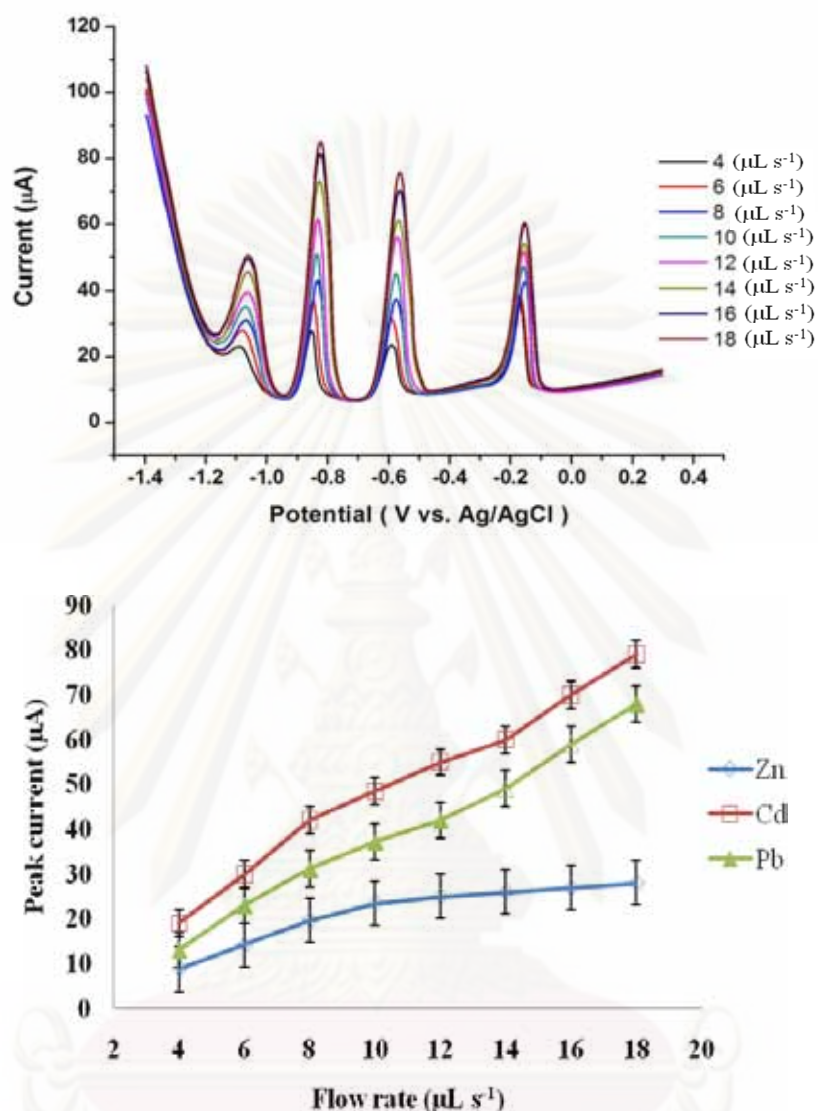**Figure 4.6** Comparison of peak height current of 50 µg L$^{-1}$ for Pb (II) and Cd (II)
and 100 µg L$^{-1}$ Zn (II) on Bi-SPCNTEs at 150 µg L$^{-1}$ of Bi (III) plating
solution at different flow rates ( 4, 6, 8, 10, 12, 14, 16 and 18 µL s$^{-1}$).
Experimental conditions;   -1.4 V of deposition potential and 180 s for
deposition time .

The stripping peak currents of Zn (II) slowly increased above 12 $\mu L\,s^{-1}$. Therefore, a flow rate of 12 $\mu L\,s^{-1}$ was selected for high sensitivity, good reproducibility, and lower consumption of the sample and the reagents.

## 4.4 Analytical Performance of the Bi-SPCNTE

Under the optimal conditions, the relationship between anodic stripping peak currents and the concentration of Pb (II), Cd (II), and Zn (II) was investigated using on-line SIA-ASV. The linearity was found to be 2-100 $\mu g\,L^{-1}$ for Pb (II) and Cd (II) and 12-100 $\mu g\,L^{-1}$ for Zn (II). Calibration curves of Pb (II) and Cd (II) have two different ranges from 2 to 18 $\mu g\,L^{-1}$ (slope: 0.3889 and 0.5865 $\mu A\,\mu g^{-1}L^{-1}$, respectively) and from 20 to 100 $\mu g\,L^{-1}$ (slope: 0.6688 and 0.7990 $\mu A\,\mu g^{-1}L^{-1}$, respectively). Calibration curve of Zn (II) also has two different slopes in the range of 12-18 and 20-100 $\mu g\,L^{-1}$ (slope: 0.1750 and 0.2437 $\mu A\,\mu g^{-1}L^{-1}$, respectively). The correlation coefficients of all calibration curves were higher than 0.992. The calibration data of heavy metals were summarized in Figure 4.7.
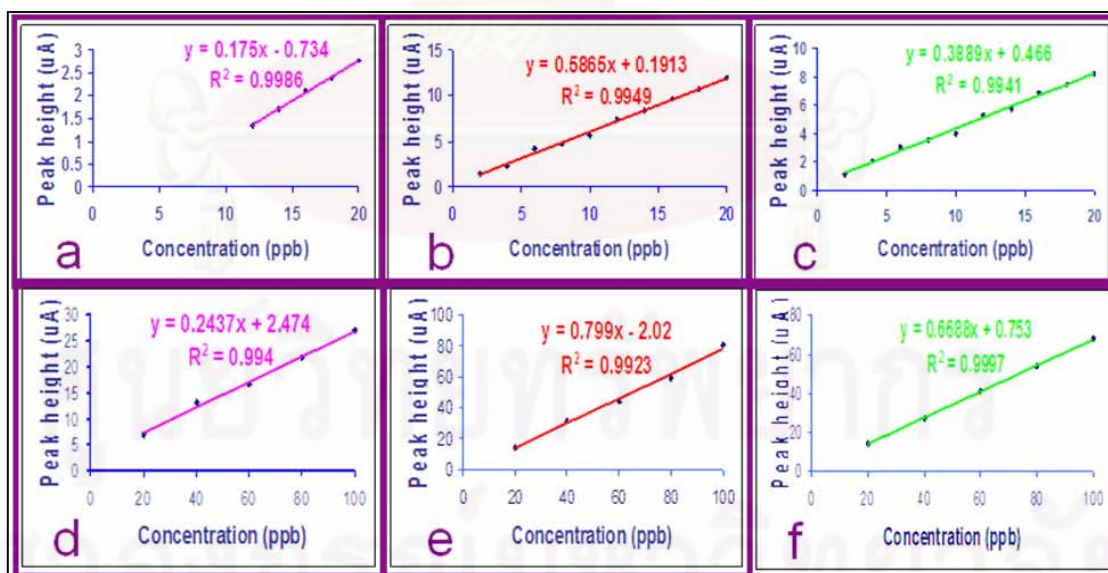


**Figure 4.7** Calibration data of heavy metals a concentration of 2-20 $\mu g\,L^{-1}$;
a: Zn, b: Cd, c: Pb and concentration of 20-100 $\mu g\,L^{-1}$ ; d: Zn,
e: Cd, F: Pb

The limits of detection (LOD) and limits of quantitation (LOQ) were calculated from $3S_{bl}/S$ and $10S_{bl}/S$, where $S_{bl}$ is the standard deviation of the blank measurement (n=10) and S is the sensitivity of the method or the slope of the linearity. LODs were 0.2 µg L$^{-1}$ for Pb (II), 0.8 µg L$^{-1}$ for Cd (II) and 11 µg L$^{-1}$ for Zn (II). The LOD and LOQ were summarized in Table 4.1.

.

**Table 4.1** LOD and LOQ of Pb (II), Cd (II) and Zn (II)

| LOD (µg L$^{-1}$) | | | LOQ (µg L$^{-1}$) | | |
|---|---|---|---|---|---|
| Pb (II) | Cd (II) | Zn (II) | Pb (II) | Cd (II) | Zn (II) |
| 0.2 | 0.8 | 11 | 3.35 | 3.46 | 26.77 |

A comparison between voltammetric response from the previous reports and our work for the simultaneous determination of Pb (II), Cd (II), and Zn (II) is summarized in Table 4.2.

**Table 4.2** Comparison of the analytical performance of electrochemical method for the determination of heavy metals.

| Electrode | Technique | System | Limits of detection (µg L$^{-1}$) | | | Number of samples per hour | Reference |
|---|---|---|---|---|---|---|---|
| | | | Pb(II) | Cd(II) | Zn(II) | | |
| Hg-multi-walled Carbon nanotubes electrode | Potentiometric stripping analysis | Batch | 6.6 | 8.4 | 28.0 | - | [13] |
| Bi-SPCE | SIA-ASV | Automatic | 0.89 | 0.69 | - | 12 | [16] |
| Bi-SPCNTE | ASV | Batch | 1.3 | 0.7 | 12 | - | [17] |
| CNT nanoelectrode array | Voltammetry | Batch | 0.04 | 0.04 | - | - | [18] |
| Bi-SPCNTE | SIA-ASV | Automatic | 0.2 | 0.8 | 11 | 14 | This work |

The detection limits of Pb (II) obtained from the developed method is 4.5-6 times lower than the previous reports using Bi film modified screen-printed carbon electrode [15,16]. Although the detection limits of Cd (II) obtained from proposed electrodes (Bi-SPCNTEs) are not significantly different from Bi-SPCEs but the proposed method has accomplished to improve the sensitivity of Zn (II) in relation to use previous automatic system [15]. This can be suggested that the use of this nanostructured material could be an alternative electrochemical sensor for the simultaneous determination of Pb (II), Cd (II), and Zn (II) in various samples whereas it would not be possible for using only carbon electrode. High reproducibility was indicated from the low relative standard deviations (lower 4%, n=6) of heavy metal ions analysis. The results are shown in Table 4.3.

**Table 4.3** Relative standard deviations (%RSD) of heavy metals.

| Heavy metals | %RSD |
|---|---|
| Pb(II) | 1.11 |
| Cd(II) | 1.88 |
| Zn(II) | 3.74 |

The result obtained showed that out method is usefulness for the simultaneous determination of Pb (II), Cd (II), and Zn (II) with low detection limits, fast analysis, and automatic system.

## 4.5    Analytical Applications

To present the valuableness of the proposed method, we applied methodology for the simultaneous determination of trace amounts of Pb (II), Cd (II) and Zn (II) in A. paniculata from leaves and capsules samples using the standard addition method. Standard addition was chosen because the matrix effects are less influenced by this procedure and it allows for compensation for proportional systematic errors. Moreover, we also optimized the ratios of acid ($HNO_3$:$HClO_4$) for A. paniculata leaves sample digestion.  Each point was the mean of the values obtained from 3 times repeated with the same electrode.  The results are shown in Table 4.4 .

**Table 4.4** Comparison of acid digestion for the determination of heavy metals by SIA-SWASV.

| Ratio of $HNO_3$:$HClO_4$ (v/v) | Zn(II) | | | Cd(II) | | | Pb(II) | | |
|---|---|---|---|---|---|---|---|---|---|
| | Slope | $R^2$ | % recovery | Slope | $R^2$ | % recovery | Slope | $R^2$ | % recovery |
| 5 : 0 | - | - | - | 0.6276 | 0.9815 | 94.88-104.90 | 0.6236 | 0.9789 | 94.20-104.20 |
| 4 : 1 | 0.1018 | 0.9471 | 86.07-108.60 | 0.5738 | 0.9733 | 92.27-105.70 | 0.5540 | 0.9914 | 94.63-103.70 |
| 3 : 2 | 0.2050 | 0.9912 | 97.30-105.13 | 0.4274 | 0.9919 | 96.14-104.18 | 0.3997 | 0.9909 | 97.20-102.85 |
| 2.5 : 2.5 ( 1:1) | 0.1233 | 0.9907 | 97.70-105.28 | 0.4622 | 0.9932 | 96.88-103.96 | 0.3628 | 0.9934 | 96.00-102.80 |
| 2 : 3 | 0.0155 | 0.9722 | 90.53-109.85 | 0.4468 | 0.9738 | 91.77-109.40 | 0.4634 | 0.9767 | 91.17-106.53 |
| 1 : 4 | 0.0924 | 0.9253 | 91.23-105.20 | 0.5722 | 0.9828 | 96.51-104.62 | 0.5135 | 0.9935 | 98.90-103.40 |
| 0 : 5 | - | - | - | 0.6253 | 0.9821 | 95.87-106.60 | 0.6353 | 0.9878 | 95.20-103.40 |

It can be observed that the optimal ratio of acid mixture for the simultaneous determination of Pb (II), Cd (II) and Zn(II) was selected at ratio of 3:2 (v/v) $HNO_3$:$HClO_4$ providing the suitable sensitivity for all of metals. In addition, we also considered the range of percentage recovery.  It was found that using the selected ratio of acid mixture offered the satisfactory recovery (96-105%) for all metals.

Typically, Pb (II) and Cd (II) have more deleterious effect on human beings using these herb items compared to Zn (II). Thus, in this work, we focused on the simultaneous determination of Pb (II) and Cd (II) in real samples. To validate the method, the results were compared with those obtained by ICP-AES. A paired t-test with 5 degrees of freedom was performed on the data obtained. The experimental t-values between the two pairs of methods were 0.1667 for Pb (II) and 1.043 for Cd (II). Statistical analysis revealed that the t-value for 5 degrees of freedom at the 95% confidence interval (2.306) was significantly higher than the above-mentioned experimental t-values. These illustrated that there are absence of statistical differences for the results obtained by the two methodologies for the determination of Pb (II) and Cd(II), t-Test data are shown in Table 4.5.

**Table 4.5** t-Test: Two-Sample Assuming Equal Variances.

|  | Variable 1 | | Variable 2 | |
|---|---|---|---|---|
|  | Cd (II) | Pb (II) | Cd (II) | Pb (II) |
| Mean | 48.748 | 39.692 | 44.6 | 38.6 |
| Variance | 52.21467 | 102.64097 | 26.8 | 109.3 |
| Observations | 5 | 5 | 5 | 5 |
| Pooled Variance | 39.507335 | 105.970485 | | |
| Hypothesized Mean Diffe | 0 | 0 | | |
| df | 8 | 8 | | |
| t Stat | 1.043445774 | 0.16772592 | | |
| P(T< =t) one-tail | 0.16362222 | 0.435480694 | | |
| t Critical one-tail | 1.859548033 | 1.859548033 | | |
| P(T< =t) two-tail | 0.327244441 | 0.870961388 | | |
| t Critical two-tail | 2.306004133 | 2.306004133 | | |

This indicates that the measurements are successful and suggesting that these results are reliable and acceptable.

# CHAPTER V

# CONCLUSIONS

## 5.1 Conclusions

From the recent literature survey it is clear that the scope for sequential injection speciation analysis is still wide open. This discontinuous nature of sequential injection analysis with its robustness, simplicity, ease of operation, reliability, low reagent and sample consumption, convenience with which sample and reagent maniputation can be automated make it ideally suitable for on-line process speciation analysis especially where process or environmental monitoring is necessary. It is sure that with the increase in speciation.

The first time the coupling of Bi-SPCNTE and automated SIA-ASV. Such proposed method provides rapid, low-cost, and highly sensitive quantitation method for Pb (II), Cd (II), and Zn (II). SPCNTEs exhibit superior sensitivity for heavy metals detection to SPCEs. The detection limits of our method using Bi-SPCNTEs ($S_{bl}/S=3$) were lower than the previous method using Bi-SPCEs. An automated SIA-ASV coupled with Bi-SPCNTE can analyze 14 samples h$^{-1}$ with high precision and low sample consumption over manual and/or batch analysis method. The proposed method was successfully ascertained via determination of µg L$^{-1}$ concentration levels of Pb (II), Cd (II) and Zn (II) in *A. paniculata* items collected from south area in Thailand.

## 5.2 Suggestion

It is known that the activity of screen-printed electrode is greatly dependent on the percentages of CNTs per carbon ink. Various amount of CNTs used in the preparation of screen-printed electrode will be investigated to obtain the optimized metal loading on CNT. In this study, the real samples studied were only *A paniculata* samples, other samples should be of particular interest for this study as well. Moreover, the proposed method can be developed for determination of other metals.
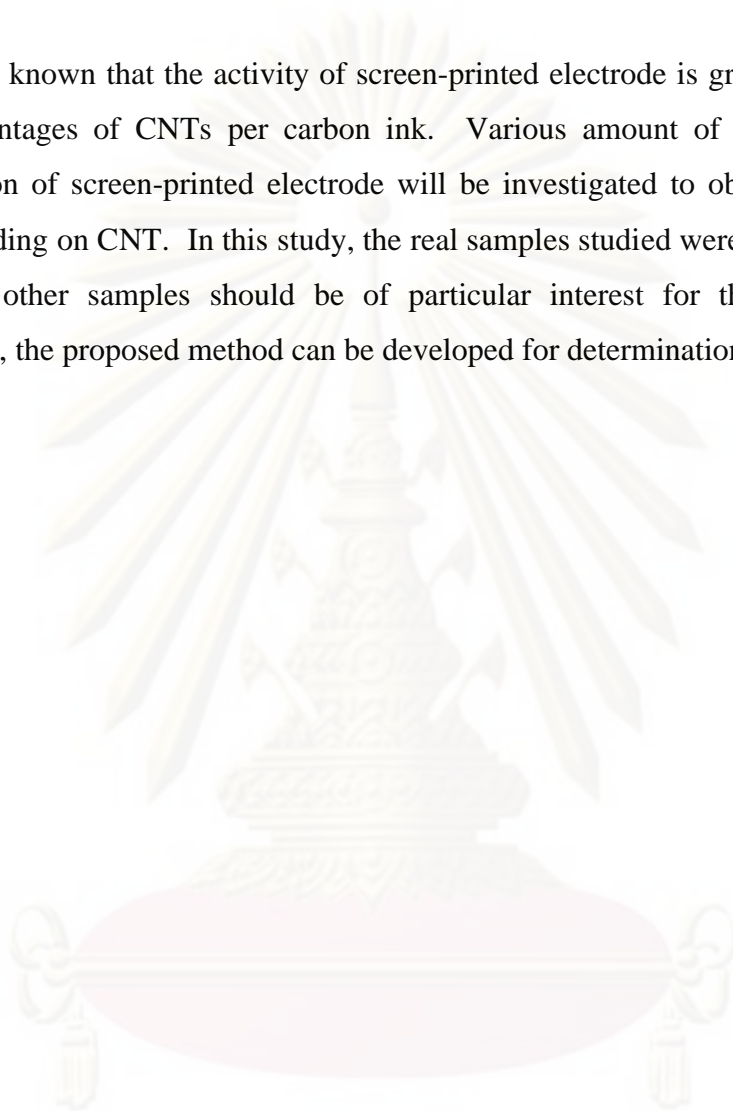
# REFERENCES

[1] He, X.; Li-ping, Z.; Su-Jie, X.; Yue-Zhong, X.; and Li-Tong, J. Nafion-coated bismuth film electrodes for the determination of trace lead and cadmium in herbal medicines by anodic stripping voltammetry. **Chin. J. Chem.** 26 (2008): 847-853.

[2] Surme, Y.; Narin I.; Soylak, M.; and Dogan, M. Determination of Lead (II) in Sediment and Water Samples. **Microchim. Acta** 157 (2007): 193-199.

[3] Tuzen, M.; and Soylak, M. Multi-element coprecipitation for separation and enrichment of heavy metal ions for their flame atomic absorption spectrometric determinations. **J. Hazard. Mater.** 162 (2009): 724-729.

[4] Horvotha, Z.S.; Lostutya, A.; Meszorosb, E.; and Molnor, A. Determination of trace metals and speciation of chromium ions in atmospheric precipitation by ICP-AES and GFAAS. **Talanta** 41 (1994): 1165-1168.

[5] Hutton, E.A.; van Elteren, J.T.; Ogorevc, B.; and Smyth, M.R. Validation of bismuth film electrode for determination of cobalt and cadmium in soil extracts using ICP-MS. **Talanta** 63 (2004): 849-855.

[6] Arpadjan, S.; Celix, G.; Taskesen, S.; and Gucer, S. Arsenic, cadmium and lead in medicinal herbs and their fractionation. **Food Chem. Toxicol.** 46 ( 2008): 2871-2875.

[7] Muntyanu, G.G. Electroanalytical properties of a thin-film mercury-carbon electrode of subnanometric thickness in high-speed linear-sweep anodic stripping voltammetry as exemplified by the determination of Zn(II), Cd(II), and Pb(II). **J. Anal. Chem.** 59 (2004): 760-767.

[8] Kefala, G.; Economou, A.; Voulgaropoulos, A.; and Sofoniou, M. A study of bismuth - film electrodes for the detection of trace metals by anodic stripping voltammetry and their application to the determination of Pb and Zn in tapwater and human hair. **Talanta** 61 (2003): 603-610.

[9] Wang, J.; Lu,J.; Hocevar, S.B.; and Farias, P.A.M. Bismuth-coated carbon electrodes for anodic stripping voltammetry. **Anal. Chem.** 72 (2000): 3218-3222.

[10] Economou, A.; and Voulgaropoulos, A. On-line stripping voltammetry of trace metals at a flow-through bismuth-film electrode by means of a hybrid flow-injection/sequential-injection system. **Talanta** 71 (2007): 758-765.

[11] Kefala, G.; and Economou, A. Polymer-coated bismuth film electrodes for the determination of trace metals by sequential-injection analysis/anodic stripping voltammetry. **Anal. Chim. Acta** 576 (2006): 283-289.

[12] van Staden, J.F.; and Stefan, R.I. Chemical speciation by sequential injection analysis: an overview. **Talanta** 64 (2004): 1109-1113.

[13] Tarley, C.R.T.; Santos, V.S.; Baeta, B.E.L.; Pereira, A.C.; and Kubota, L.T., Similtaneous determination of zinc, cadmium and lead in environmental water samples by potentiometric stripping analysis (PSA) using multiwalled carbon nanotube electrode. **J. Hazard. Mater.** 169 (2009): 256-262.

[14] Hutton, E.A.; Hocevar, S.B.; Mauko, L.; and Ogorevc, B., Bismuth film electrode for anodic stripping voltammetric determination of tin. **Anal.Chim. Acta** 580 (2006): 244-250.

[15] Chuanuwatanakul, S.; Dungchai, W.; Chailapakul, O.; and Motomizu, S., Determination of trace heavy metals by sequential injection-anodic stripping voltammetry using bismuth film screen-printed carbon electrode. **Anal. Sci.** 24 (2008): 589-594.

[16] Hwang, G.H.; Han, W.K.; Park, J.S.; and Kang, S.G., Determination of trace metals by anodic stripping voltammetry using a bismuth-modified carbon nanotube electrode. **Talanta** 76 (2008): 301-308.

[17] Liu, G.; Lin, Y.; Tu, Y.; and Ren, Z., Ultrasensitive voltammetric detection of trace heavy metal ions using carbon nanotube nanoelectrode array. **Analyst** 130 (2005): 1098-1101.

[18] Wang, J.; Lu,J.; Kigoz, U.A.; Hocevar, S.B.; and Ogoreve, B., Insights into the anodic stripping voltammetric behavior of bismuth film electrodes. **Anal.Chim. Acta.** 434 (2001): 29-34.

[19] Kaim W,; Schwederski B. **Bioinorg. Chem. Appl.** 1st ed. New York : John Wiley& Sons; 1994.

[20] Sawyer, D.T.; Sobkowiak, A.; and Robert, J.L. **Electrochemistry for Chemists**. New York: Wiley Interscience; 1995.

[21] Settle, F.A. **Handbook of Instrumental Techniques for Analytical Chemistry**. New Jersey: Prentice Hall; 1997.

[22] Thomas, F.G.; and Henze, G. **Introduction to Voltammetric Analysis**. Collingwood, Australia: CSIRO Publishing; 2001.

[23] Christian, G. D.; and O'Reilly, J. E. **Instrument Analysis**. 2nd ed: Allyn and Eacon; 1978.

[24] Skoog, D. A.; Holler, F. J.; and Nieman, T. A. **Principles of Instrument Analysis.** New York, USA: Harcourt Brace College Publishers; 1998.

[25] Braun, R. D. **Introduction to Instrumental Analysis.** Singapore: McGraw-Hill Book; 1987.

[26] Vasile, V.N. On the performance of supercapacitors with electrodes based on carbon nanotubes and activated material. **Phys. Rev. E** 40 (2008): 2596-2605.

[27] Jiang, Q.; Qu, M.; Zhou, G.; and Zhang, B. A study of activated carbon nanotubes as electrochemical super capacitor electrode materials. **Materials Letters** 57 (2002): 988-991.

[28] Chen, Q.; Xu, R.; and Yu, D. Multiwalled carbon nanotube/polybenzoxazine nanocomposites: Preparation, characterization and properties. **Polymer** 47 (2006): 7711-7719.

[29] Catalytic Synthesis of Carbon Nanotubes. **What are Carbon Nanotubes** [online]. n.d. Available from: http://cobweb.ecn.purdue.edu/~catalyst/ Carbon%20Nanotubes/Catalytic%20Nanotubes/Catalytic%20Synthesis% 20of%20Carbon%20Nanotubes.htm [2008, March 24]

[30] Tangkuaram, T.; Ponchio, C.; Kangkasomboon, T.; Katikawong, P.; and Veerasai, W. Design and development of a highly stable hydrogen peroxide biosensor on screen printed carbon electrode based on horseradish peroxidase bound with gold nanoparticles in the matrix of chitosan. **Biosens. Bioelectron.** 22 (2007): 2071-2078.

[31] Economou, A.  Sequential-injection analysis (SIA):  A  useful  tool  for on-line sample-handling  and  pre-treatment. **TrAC, Trends Anal. Chem.** 24 (2005): 416-425.

[32] Ruzicka, J.; and Hansen, E.H.  Flow injection analyses: Part I.  A new concept of fast continuous flow analysis. **Anal. Chim. Acta** 78 (1975): 145-157.

[33] Stewart, K. K.;  Beecher, G.R.;  and Hare, P. E.  Rapid analysis of discrete samples: The use of nonsegmented,  continuous flow. **Anal. Biochem.** 70 (1976): 167-173.

[34] Perez-Olmos,  R.; Soto, J. C.;  Zarate, N.;  Araujo, A. N.; and Montenegro, M. C. B. S. M.  Sequential  injection analysis using electrochemical detection: A review. **Anal. Chim. Acta** 554 (2005): 1-16.

[35] Barnett, N.W.; Lenehan, C. E.; and Lewis, S.W. Sequential injection analysis: an alternative  approach to  process analytical chemistry. **TrAC, Trends Anal. Chem.** 18 (1999): 346-353.

[36] Ruzicka, J.; and Marshall, G. D. Sequential injection: a new concept for chemical sensor,  process  analysis  and  laboratory  assays. **Anal. Chim. Acta** 237 (1990): 329-343.

[37] Marshall,  G.;  Wolcott,   D.; and Olson, D. Zone fluidics in flow  analysis: potentialities and applications. **Anal. Chim. Acta** 499 (2003): 29-40.

[38] Wang, Z.; Liu, J.; Liang, Q.; Wang, Y.; and Luo, G. Carbon nanotube-modified electrodes  for  the  simultaneous  determination of dopamine and ascorbic acid. **Analyst** 127 (2002): 653–658.

[39] Knupp, S.L.; Li, W.;  Paschos, O.; Murray, T.M.; Snyder, J.; and Haldar, P.  The effect  of  experimental  parameters  on  the  synthesis  of  carbon nanotube/nanofiber supported  platinum by  polyol processing techniques. **Carbon**  46 (2008): 1276–1284.

[40] Chen, J.; Wang, M.; Liu, B.; Fan, Z.; Cui, K.; and Kuang, Y. Platinum catalysts prepared  with  functional  carbon  nanotube  defects  and  its  improved catalytic  performance  for  methanol  oxidation. **J. Phys. Chem. B** 110 (2006): 11775–11779.

[41] Wang, H.J.; Zhou, A.L.; Peng, F.; Yu, H.; and Chen, L.F. Adsorption characteristic of acidified carbon nanotubes for heavy metal Pb(II) in aqueous solution. **Mater. Sci. Eng., A** 466 (2007): 201-206.

[42] Stafiej, A.; and Pyrzynska, K. Adsorption of heavy metal ions with carbon nanotubes. **Sep. Purif. Technol.** 58 (2007): 49-52.

[43] Wang, H.; Zhou, A.; Peng, F.; Yu, H.; and Yang, J. Mechanism study on adsorption of acidified multiwalled carbon nanotubes to Pb(II). **J. Colloid Interface Sci.** 316 (2007): 277-283.

# APPENDIX

**Table 4.6** Peak height for the comparison of the electrochemical response between Bi-SPCNTEs and Bi-SPCEs.

| Concentration of Bi(III) ($\mu gL^{-1}$) | Peak height ($\mu A$) | | | | | |
|---|---|---|---|---|---|---|
| | Zn(II) | | Cd(II) | | Pb(II) | |
| | CNT | C ink | CNT | C ink | CNT | C ink |
| 10 | 5.01 | ND | 33.20 | 15.05 | 31.21 | 25.20 |
| 30 | 12.10 | ND | 39.89 | 32.40 | 45.12 | 40.50 |
| 50 | 21.32 | 5.12 | 52.97 | 44.21 | 55.89 | 42.50 |
| 80 | 32.10 | 13.45 | 56.02 | 48.87 | 63.45 | 51.95 |
| 100 | 37.57 | 17.98 | 58.21 | 50.25 | 69.80 | 52.02 |
| 200 | 44.89 | 26.22 | 62.02 | 52.32 | 70.09 | 56.03 |
| 300 | 49.98 | 27.50 | 65.32 | 53.50 | 75.34 | 59.95 |

**Table 4.7** Peak height for the comparison of percentages of CNTs to carbon ink : Zn(II).

| Concentration of Bi(III) ($\mu gL^{-1}$) | Peak height ($\mu A$) | | |
|---|---|---|---|
| | 5%v/v | 10%v/v | 15%v/v |
| 50 | 12.00 | 5.03 | ND |
| 100 | 21.09 | 13.85 | 8.50 |
| 150 | 24.95 | 18.05 | 11.20 |
| 200 | 30.02 | 22.95 | 7.54 |
| 250 | 26.05 | 18.10 | 5.01 |
| 300 | 25.02 | 16.90 | 4.32 |

**Table 4.8** Peak height for the comparison of percentages of CNTs to carbon ink :
Cd(II).

| Concentration of Bi(III) ($\mu gL^{-1}$) | Peak height ($\mu$A) | | |
|---|---|---|---|
| | 5%v/v | 10%v/v | 15%v/v |
| 50 | 32.20 | 35.00 | 35.00 |
| 100 | 57.50 | 39.20 | 36.50 |
| 150 | 60.00 | 44.80 | 32.50 |
| 200 | 61.90 | 47.50 | 34.02 |
| 250 | 67.50 | 44.90 | 27.04 |
| 300 | 70.03 | 41.52 | 24.02 |

**Table 4.9** Peak height for the comparison of percentages of CNTs to carbon ink :
Pb(II).

| Concentration of Bi(III) ($\mu gL^{-1}$) | Peak height ($\mu$A) | | |
|---|---|---|---|
| | 5%v/v | 10%v/v | 15%v/v |
| 50 | 35.00 | 30.00 | 27.50 |
| 100 | 55.00 | 30.52 | 29.03 |
| 150 | 57.04 | 44.03 | 27.52 |
| 200 | 58.50 | 47.02 | 25.75 |
| 250 | 65.00 | 49.82 | 23.95 |
| 300 | 67.02 | 47.50 | 13.02 |

**Table 4.10** Peak height for effect of bismuth plating solution concentration.

| Concentration of Bi(III) ($\mu gL^{-1}$) | Peak height ($\mu A$) | | |
|---|---|---|---|
| | Zn(II) | Cd(II) | Pb(II) |
| 10 | 2.16 | 25.50 | 38.40 |
| 50 | 4.12 | 33.30 | 40.20 |
| 100 | 15.00 | 41.02 | 40.20 |
| 150 | 21.01 | 45.20 | 40.10 |
| 200 | 26.85 | 49.80 | 40.50 |
| 250 | 27.70 | 55.40 | 45.50 |
| 300 | 25.50 | 55.20 | 46.20 |

**Table 4.11** Peak height for effect of deposition time.

| Deposition time (s) | Peak height ($\mu A$) | | |
|---|---|---|---|
| | Zn(II) | Cd(II) | Pb(II) |
| 60 | 4.90 | 17.00 | 13.01 |
| 90 | 8.70 | 28.50 | 23.05 |
| 120 | 17.20 | 43.05 | 33.50 |
| 150 | 22.00 | 55.02 | 48.30 |
| 180 | 22.09 | 56.90 | 51.50 |
| 210 | 23.00 | 57.50 | 52.50 |
| 240 | 23.02 | 57.90 | 53.95 |
| 270 | 23.08 | 58.04 | 54.50 |
| 300 | 23.10 | 65.02 | 60.90 |

**Table 4.12** Peak height for effect of flow rate.

| Flow rate ($\mu Ls^{-1}$) | Peak height ($\mu A$) | | |
|---|---|---|---|
| | Zn(II) | Cd(II) | Pb(II) |
| 4 | 8.84 | 18.90 | 15.20 |
| 6 | 14.20 | 29.90 | 23.00 |
| 8 | 19.70 | 39.70 | 31.10 |
| 10 | 23.50 | 48.50 | 37.20 |
| 12 | 27.20 | 57.20 | 44.50 |
| 14 | 29.80 | 65.80 | 53.00 |
| 16 | 32.80 | 73.80 | 61.90 |
| 18 | 33.50 | 77.40 | 67.50 |

**Table 4.13** Peak height for analytical performance of the Bi-SPCNTEs ;(LOD, LOQ).

| N | Peak height ($\mu A$) | | |
|---|---|---|---|
| | Zn(II) | Cd(II) | Pb(II) |
| 1 | 16.5 | 11.8 | 12.8 |
| 2 | 16.7 | 11.4 | 12.5 |
| 3 | 17.0 | 11.5 | 12.4 |
| 4 | 17.2 | 11.6 | 12.6 |
| 5 | 17.3 | 11.8 | 12.7 |
| 6 | 17.2 | 11.4 | 12.4 |
| 7 | 16.7 | 11.6 | 12.7 |
| 8 | 16.5 | 11.8 | 12.5 |
| 9 | 16.2 | 11.1 | 12.2 |
| 10 | 16.3 | 11.5 | 12.5 |

**Table 4.14** Peak height for analytical performance of the Bi-SPCNTEs ; (%RSD).

| N | Peak height (µA) | | |
|---|---|---|---|
| | **Zn(II)** | **Cd(II)** | **Pb(II)** |
| 1 | 10.00 | 19.60 | 17.60 |
| 2 | 9.81 | 19.30 | 17.40 |
| 3 | 9.75 | 19.10 | 17.30 |
| 4 | 10.30 | 19.60 | 17.50 |
| 5 | 9.92 | 20.10 | 17.60 |
| 6 | 9.19 | 19.20 | 17.10 |

**Table 4.15** Peak height for linear range at low concentration.

| Concentrations ($\mu gL^{-1}$) | Peak height (µA) | | |
|---|---|---|---|
| | **Zn(II)** | **Cd(II)** | **Pb(II)** |
| 2 | ND | 1.43 | 1.12 |
| 4 | ND | 2.33 | 2.08 |
| 6 | ND | 4.23 | 3.04 |
| 8 | ND | 4.65 | 3.57 |
| 10 | ND | 5.66 | 4.01 |
| 12 | 1.35 | 7.44 | 5.31 |
| 14 | 1.72 | 8.36 | 5.78 |
| 16 | 2.10 | 9.62 | 6.90 |
| 18 | 2.40 | 10.76 | 7.46 |

**Table 4.16** Peak height for linear range at high concentration.

| Concentrations ($\mu gL^{-1}$) | Peak height ($\mu A$) | | |
|:---:|:---:|:---:|:---:|
| | **Zn(II)** | **Cd(II)** | **Pb(II)** |
| 20 | 6.88 | 14.30 | 14.14 |
| 40 | 13.20 | 31.60 | 27.23 |
| 60 | 16.70 | 44.10 | 41.47 |
| 80 | 21.70 | 59.20 | 53.84 |
| 100 | 27.00 | 80.40 | 67.71 |

**Table 4.17** Acceptable RSD values according to AOAC International.

| Analyte % | Analyte ratio | Unit | RSD(%) |
|:---:|:---:|:---:|:---:|
| 100 | 1 | 100% | 1.3 |
| 10 | $10^{-1}$ | 10% | 2.8 |
| 1 | $10^{-2}$ | 1% | 2.7 |
| 0.1 | $10^{-3}$ | 0.1% | 3.7 |
| 0.01 | $10^{-4}$ | 100 ppm | 5.3 |
| 0.001 | $10^{-5}$ | 10 ppm | 7.3 |
| 0.0001 | $10^{-6}$ | 1 ppm | 11 |
| 0.00001 | $10^{-7}$ | 100 ppb | 15 |
| 0.000001 | $10^{-8}$ | 10 ppb | 21 |
| 0.0000001 | $10^{-9}$ | 1 ppb | 30 |

**Table 4.18** Acceptable recovery percentages as a function of the analyte concentration.

| Analyte % | Analyte ratio | Unit | Mean recovery (%) |
|---|---|---|---|
| 100 | 1 | 100% | 98-102 |
| 10 | $10^{-1}$ | 10% | 98-102 |
| 1 | $10^{-2}$ | 1% | 97-103 |
| 0.1 | $10^{-3}$ | 0.1% | 95-105 |
| 0.01 | $10^{-4}$ | 100  ppm | 90-107 |
| 0.001 | $10^{-5}$ | 10  ppm | 80-110 |
| 0.0001 | $10^{-6}$ | 1  ppm | 80-110 |
| 0.00001 | $10^{-7}$ | 100  ppb | 80-110 |
| 0.000001 | $10^{-8}$ | 10  ppb | 60-115 |
| 0.0000001 | $10^{-9}$ | 1  ppb | 40-120 |

# VITA

**Name**               :    Miss Uthaitip  Injang

**Date of Birth**      :    Jan 18, 1975

**Place of Birth**     :    Trang, Thailand

**Graduated**          :    1994–1998    Bachelor Degree of Science

(Chemistry), Taksin University

2007–2010    Master Degree of Science Program in

Analytical Chemistry,

Chulalongkorn University

**Home address:**            6, Moo 5, Tambol Sawiat, Amphur Thachang,

Surattanee 84150, Thailand

**Poster Presentation** :    2009         Symposium on Flow Based Analysis

2009, ChiangMai, Thailand.

2009         Flow analysis XI, Pollensa Mallorca,

Spain

**Publication**              2010         "Determination of trace heavy metals in

herbs by sequential injection analysis-

anodic stripping voltammetry using

screen-printed carbon nanotubes

electrodes" Analytica chimica Acta

668 (2010) 54-60.